The d' Alembert-Lagrange principal equations and applications to floating flexible systems

Kwang-Chun Park, Carlos A. Felippa, Roger Ohayon

The d'Alembert–Lagrange principal equations and applications to floating flexible systems

K. C. Park[1,*,†], Carlos A. Felippa[1] and Roger Ohayon[2]

[1]*Center for Aerospace Structures, University of Colorado, Boulder, CO 80309-0429, U.S.A.*
[2]*Structural Mechanics and Coupled Systems Laboratory, Conservatoire National des Arts et Metiers (CNAM), C.C. 353, 292 rue Saint-Martin, 75141 Paris Cedex 03, France*

This paper addresses the dynamics and quasi-statics of floating flexible structures as well as extensions to unconstrained substructures and partitions of coupled mechanical systems. The *principal solution* is defined as the state of self-equilibrated forces obtained as the particular solution of the rigid motion and interface equilibrium equations. This solution is independent of the stress–strain constitutive properties as well as of the compatibility equations. For statically determinate systems, the principal solution is the final force solution. For statically indeterminate systems, the correction due to flexibility and compatibility is orthogonal to the principal solution. The formulation is done in the context of d'Alembert's principle, which supplies the *d'Alembert–Lagrange principal equations* for floating bodies. These are obtained by summation of virtually working forces and moments acting on the floating systems. Applications of this approach are demonstrated on a set of dynamic and quasi-static example problems of increasing generality. Linkage to variational principles with an interface potential is eventually discussed as providing the theoretical foundation for handling interacting semi-discrete subsystems linked by node-collocated Lagrange multipliers.

KEY WORDS: dynamics; d'Alembert's principle; floating systems; principal equations; Lagrange multipliers; partitioned analysis

1. INTRODUCTION

In presentations dealing with motions of fully unconstrained fluid and solid systems, the authors have often been asked whether a floating, flexible body under dynamic loads is in an equilibrium state, or whether an unsupported structure such as a flying aircraft maintains equilibrium as it moves and deforms. Doubts on such a fundamental subject suggest a gap in the teaching of classical

*Correspondence to: K. C. Park, Center for Aerospace Structures, University of Colorado, Boulder, CO 80309-0429, U.S.A.
†E-mail: kcpark@colorado.edu

dynamics, as well as difficulties in the appropriate translation of basic concepts of Newtonian physics to computational mechanics.

The main purpose of this paper is to clarify several aspects of the subject by emphasizing the role played by what we call the *d'Alembert–Lagrange principal equations* in the context of the dynamics of unconstrained flexible bodies. The gap noted above may be due to increasing specialization in the teaching of various flavors of engineering, as discussed subsequently. In order to set the scope of the paper, a *floating*, *flexible body* in the present paper is defined not to contain internal mechanisms such as sliding and rotating links, as well as elemental spurious mechanisms in the context of finite element methods. Principal equations for systems with internal mechanisms are only briefly addressed as their derivation remains a case-by-case challenge, the detailed analysis of which would significantly lengthen the exposition. Nevertheless, we believe that the essential physics of the d'Alembert–Lagrange principal equations can be revealed and explained to the reader without being drawn into intricate features involving internal mechanisms.

Traditional education in civil and mechanical engineering has focused on motion-controlled systems. Engineers in those majors are trained early during the undergraduate curriculum on how to apply sufficient support conditions to preclude unsafe motions. They are taught to design restraints to permit only controlled motions as in a vehicle rolling, a washing machine cycling, a bascule bridge folding, or a crane lifting a load. By contrast, fully unconstrained systems are more common in aerospace engineering, which deals with things such as flying aircraft, staging rockets, and orbiting satellites. Aerospace structural engineers learn how to cope with the inherent lack of stability of such systems in the framework of *dynamics* by learning topics such as guidance and attitude control.

Recent advances in the model-based simulation of complex mechanical systems have introduced a new ingredient of computational nature. A complex, FEM-discretized mechanical system may be divided into subsystems for modeling or computational reasons. Such subsystems are variously called substructures, super-elements, or subdomains according to the context in which the decomposition or partitioning is done. If subsystems are connected by interaction forces, some may be unconstrained when viewed as individual entities. Think of the Eiffel Tower horizontally sliced into several substructures: only those pieces connected to the leg foundations will be kinematically restrained, whereas the others will be unconstrained against rigid motions before interaction conditions are set up. Qualifiers used in the mechanics literature for bodies or structures at liberty against rigid motions vary. They include *floating*, *free–free*, *completely free*, *unrestrained*, *fully unsupported* and *rigid-motion-unconstrained*. In this paper, we shall often use *floating* and *free–free* to evince visualization of the body moving as a whole.

A related situation arises in the partitioned analysis of coupled systems that contain heterogeneous mechanical components such as structures, soil media, or fluids. (A partition is a spatial subdivision based on physics; for example, the model of a dam excited by seismic motions might be divided into a fluid, a structure, and a soil partition.) If the interaction is treated through Lagrange multipliers, individual partitions become floating bodies.

The difference between genuinely floating structures such as aircraft or satellites and the computationally induced case is one of the goals. The rigid-body motions of an aircraft are controlled by a human or automatic pilot to achieve the goal of following a trajectory; that is, a physical objective. In simulations, the goal is to use such motions to fulfill a computational objective; for example, to facilitate parallel computations, to speed up iterative solution algorithms, or to expedite coupling of existing software modules.

The treatment of multiplier-connected components of a mechanical system has been addressed by many authors, particularly in the context of multibody dynamics [1], parallel computations [2, 3], and multiphysics simulations [4, 5]. From a fundamental standpoint, the most satisfactory treatments have been based on variational principles, such as those cited in the *Historical Background* section. Such 'top down' derivations; however, may seem too abstract to engineers and scientists primarily concerned about how these methods can be useful in practical applications.

The aim of this paper is to deal with floating components in a more agile, step-by-step fashion by proceeding in a 'bottom up' manner. That is, starting with simple examples, and progressing toward the general case by stages while emphasizing the physical interpretation. Although linkage to variational principles is eventually made that is not an essential part of the exposition. It may be skipped by those readers primarily interested in modeling and implementation aspects.

Aside from the general goal of clarifying 'floating flexible dynamics', the paper has three specific objectives:

- Present the principal equations for a floating body or structure in a form suitable for matrix formulation and computer implementation. Those equations *define that portion of the solution independent of constitutive properties and compatibility conditions*. Mathematically that subspace spans the particular solution of the combined rigid motion and interface equilibrium equations.
- Discuss the matrix form of the kinematic-static duality associated with the principal equations, which states that *the self-equilibrium and rigid-body-basis matrices are the transposes of each other.*
- Apply the foregoing concepts to a set of examples of increasing generality.

Beyond the classical context of multibody, guidance and attitude dynamics, rigid-body motions and thus the d'Alembert–Lagrange principal equations play increasingly important roles in emerging fields such as molecular dynamics [6–10], biophysics [11–15], as well as traditional applications such as multibody dynamics [16–19].

The quasi-static case of the principal equations and equivalent forms have been utilized in the formulation of the classical force method (CFM) [20, 21], in the development of finite elements [22, 23], in the solution of singular systems for quasi-static problems [24], in vibration eigenvalue problems [25], and for the parallel solution of large-scale structural systems [2, 3]. We believe that additional developments for multiphysics and multiscale applications remain to be done.

We emphasize that the focus of the present paper is on the d'Alembert–Lagrange principal equations (hereafter simply termed as *principal equations*), *not* on the more general d'Alembert–Lagrange equations or principles. The remainder of the paper is organized as follows.

Section 2 offers the historical background of the principal equations, from Newton to date, in the hope that the readers who are unfamiliar with the subject may want to start by reading this section while taking note of the references cited therein. It highlights roles played in the development of the force method of structural analysis, well-posedness of floating systems, subsystem interface conditions, and dual subdomain decomposition techniques for parallel computing.

In Section 3, we introduce the principal equations by way of a two-mass and three-spring plane-motion problem. It is shown that the three principal equations are obtained by summing the forces and moments. We label the force and moment summation operators as *self-equilibrium operators*. Hence, the principal equations are obtained by the projection of the governing flexible equations of motion (EOM) onto the self-equilibrium operators. We show that the self-equilibrium and system

rigid-body matrices are the transposes of each other. The section ends with a comment on an application of the self-equilibrium operators to establish solvability conditions for eigenproblems in which accelerations are prescribed.

Section 4 derives the self-equilibrium operator of a partially constrained static system, from which both the principal equations as well as conditions on admissible external forces readily emerge. Section 5 derives a general form of principal equations for partitioned linear flexible structural systems in conjunction with the method of localized Lagrange multipliers (LLM) [26–29]. Section 6 offers a step-by-step illustration of solving static partitioned floating systems by utilizing the principal equations.

Section 7 presents a discrete variational formulation of partitioned structural systems in terms of deformations, rigid-body modes (RBM), LLM, and interface frame displacements as independently varied state variables. The rigid-body mode equations are shown to conflate into the principal equations.

The Conclusions section lists potential future applications of the principal equations, with emphasis on the computational treatment of multiphysics and multiscale problems.

2. HISTORICAL BACKGROUND

This section outlines the original development of principal equations and some of their applications in classical and computational mechanics. No attempt to historical completeness is made. The reader may consult, for example, Dugas [30] or Truesdell and Toupin [31] for classical developments or Farhat and Roux [3] for uses in domain decomposition methods.

2.1. Theoretical background

In their 1960 review of field theories Truesdell and Toupin [31, p. 595] state that 'The Principle of Virtual Work (PVW), which when the reaction of inertia is included may be called the Lagrange–d'Alembert principle, is the oldest general variational form of the equations of mechanics.' Lanczos [32, p. 92] remarks that 'd'Alembert's principle gives a complete solution of problems in mechanics. All different principles of mechanics are merely mathematically different formulations of d'Alembert's principle.' [Caution: the term 'principle' is not to be interpreted in the modern sense of a true variational principle such as Hamilton's. The PVW is actually what we call now a weak form or Galerkin form, with virtual displacements as test functions.]

As a variational statement d'Alembert's principle was first proven for a fully unconstrained system of bodies by Lagrange in his *Mécanique Analytique* [33, 2de Partie, 3me Section 3]. Thus a fair attribution should include both names. For example, in a Wikipedia article [34], it is called the d'Alembert–Lagrange principle, which is chronologically appropriate.

D'Alembert's contribution to the dynamical PVW was indirect but important. He had asserted in his *Traité de Dynamique* [35, Section 50] that an accelerating system can be transformed into an equivalent static system by adding the so-called inertial force and inertial torque or moment. The inertial force must act through the center of mass whereas the inertial torque can act anywhere. (The direct application of Newton's laws requires that the angular acceleration be applied only about the center of mass.) A coordinate system in which this substitution is valid is called an inertial frame. For example, if the total mass (assumed invariant) of the system is M and the center of mass acceleration with respect to an inertial frame is $\ddot{x}$, the inertial force is $-M\ddot{x}$.

Superposing the inertial force and torque reactions to the actual external forces and moments acting on the system gives the effective forces and effective moments acting on the body. (Some authors, such as Synge [36], reserve the name 'effective forces' for the inertial part.) Lagrange [33, 2de Partie, 1re Section] observes: 'Cette méthode réduit toutes les lois du mouvement des corps à celles de leur équilibre, et ramène ainsi la Dynamique à la Statique.'

An immediate consequence is the center-of-mass theorem: If a body is mass invariant and referred to an inertial frame then the center of mass moves as a mass-point, of mass equal to the mass of the body and subject to the effective force acting on the body [31, p. 532]. This law precedes the PVW by a century. It had been used for special cases by Newton [37, Corollary III to Laws of Motion], d'Alembert [35, 38], and Euler [39]. It was shown to apply to 'un corps quelconque' by Lagrange [33, 2de Partie, 3me Section 3].

Abetting the 'territorial split' of calculus dating back to Newton and Leibnitz, Euler, and Lagrange downplayed the use of Newton's laws. The equivalence of the PVW and Lagrange's analytical dynamics to Newton's laws and conservation principles was established nearly a century later by Thomson (Lord Kelvin) and Tait [40]. Compared with Newton's laws, a major advantage of the PVW as an integral form of equations of balance is the automatic elimination of workless forces. In a continuum constrained body, the PVW does not include any stress required to maintain the constraints, as long as such stresses do not work. A classical example is the incompressibility constraint in isochoric motions. The PVW is, therefore, indeterminate with respect to workless forces or stress systems.

2.2. Substructuring, partitioning, and floating systems

Substructuring in the FEM context was introduced in the aerospace industry during the 1960s as a device to overcome resource limitations on computers of the time, as well as to stage communication between different design groups. Two flavors, based on the displacement and force methods, are well covered in [21]. For the force version, however, floating substructures were avoided *a priori*. This kind of spatial subdivision method evolved in three directions: superelements [41] for multilevel decomposition in the late 1960s, partitions [42] for coupled problems in the late 1970s, and subdomains [2, 3] for parallel processing during the 1990s.

The treatment of floating bodies in the context of matrix structural analysis was systematically addressed by Fraeijs de Veubeke [22]. Unfortunately this 1973 lecture material never appeared on a journal. Another pioneering presentation is that of Verchery [24]. The treatment of interfaces by Lagrange multipliers as connectors has older roots. As a variational principle to treat actual discontinuities in continuum (field) models, it was first proposed by Prager [43]. His principle links interface displacements through a single global Lagrange multiplier field. The idea was expanded and applied by Tong in the hybrid-FEM context [44]. It was systematically extended as a family of variational principles by Atluri [45], also with the development of hybrid FEM models in mind. Its use for parallel computation was successfully pursued by Farhat and Roux [2, 3], who used global Lagrange multipliers as subdomain connectors for structural and acoustic partitions in multiphysics applications. The use of LLM for interfacing substructures was proposed and developed in [26–29] and for fluid–structure interaction in [4, 37].

2.3. Principal equations and the CFM

There is a link between the CFM of structural analysis and the principal equations that is worth noting. The separation of the internal force state into principal and deformational states has ancient

roots in the CFM, tracing back to Maxwell, Betti, Castigliano, and Clapeyron in the XIX Century. The example of Section 3, which leads to Equations (4)–(6), plainly illustrates that idea. The CFM decomposes the solution into a primary and a redundant-driven state. The former pertains to a fictitious, statically determinate 'base' structure brought into existence by physical cuts (partitions) that activate redundants. Adjusting the redundants to meet cut (partitioned) compatibility conditions yields the correct solution by superposition. It should, however, be pointed out that very few researchers, if any, have addressed the so-called *principal* state for the dynamical problems. As narrated in [46], the chief technical difficulty that hampered the traditional approach in the computer era was the automated selection of redundancies. This obstacle has been attacked by several investigators since the mid-1960s. Notable efforts to date include the Gauss–Jordan rank technique [47], minimum-norm solutions [48, 49] suggested by the natural factor technique [50], and the integrated force method [51, 52].

2.4. A dynamic version of the force method

None of the foregoing force method variations has succeeded in the commercial FEM environment. There is a practical barrier: all of them require element reformulation in terms of flexibilities and element-by-element extraction of discrete equilibrium equations. That shift is unlikely to happen in view of the huge investment on stiffness-based element libraries as well as on element interoperability. There are also application range limitations. Unsupported mechanical systems do not possess conventional flexibilities. No dual method gracefully handles dynamic, stability, and kinematically non-linear problems, as primal methods effortlessly do. For example, treating inertial effects necessarily brings in flexibilities to pass from accelerations to forces as independent variables, entangling spurious elasticity properties into the realm of mass. We hope that the force decomposition method presented here in conjunction with LLM—as displayed, for example, in Equation (55)—forestalls those shortcomings and assists software reuse by retaining displacements and their time derivatives as primary variables.

3. A FLOATING SPRING–MASS SYSTEM

This section illustrates, through a simple example, the derivation of the principal equations for a floating system. Consider a spring–mass model of the boomerang shown in Figure 1, assumed to move in the x, y plane. [The model shown there is used only for illustrative purposes. For predicting actual motions it is totally inadequate as it lacks aerodynamic forces; furthermore, the beam stiffness of the boomerang is ignored, which leads to a spurious kinematic mode.]

The EOM are written first for a rigid system with instantaneous center of mass located at c, which is taken as origin of coordinates. Force balance in the x, y directions and momentum balance about the z direction give

$$\begin{bmatrix} \mathbf{m} & 0 \\ 0 & \mathbf{m} \end{bmatrix} \begin{Bmatrix} \ddot{\mathbf{u}} \\ \ddot{\mathbf{v}} \end{Bmatrix} + \begin{bmatrix} \mathbf{k}_x & 0 \\ 0 & \mathbf{k}_y \end{bmatrix} \begin{Bmatrix} \mathbf{u} \\ \mathbf{v} \end{Bmatrix} = \begin{Bmatrix} \mathbf{f}_x \\ \mathbf{f}_y \end{Bmatrix} \tag{1}$$

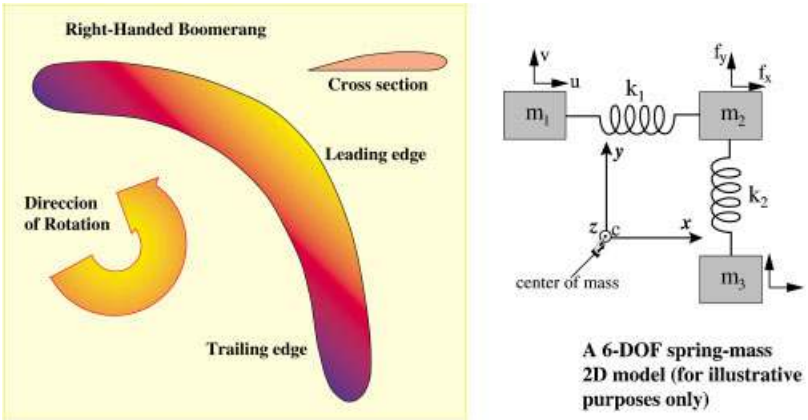

Figure 1. A crude spring-mass 2D model of a boomerang. (Note this simple model does not capture boomerang motions.)

in which

$$\mathbf{m}=\begin{bmatrix} m_1 & 0 & 0 \\ 0 & m_2 & 0 \\ 0 & 0 & m_3 \end{bmatrix},\quad \mathbf{k}_x=\begin{bmatrix} k_1 & -k_1 & 0 \\ -k_1 & k_1 & 0 \\ 0 & 0 & 0 \end{bmatrix},\quad \mathbf{k}_y=\begin{bmatrix} 0 & 0 & 0 \\ 0 & k_2 & -k_2 \\ 0 & -k_2 & k_2 \end{bmatrix}$$
$$\mathbf{u}=\begin{Bmatrix} u_1 \\ u_2 \\ u_3 \end{Bmatrix},\quad \mathbf{v}=\begin{Bmatrix} v_1 \\ v_2 \\ v_3 \end{Bmatrix},\quad \mathbf{f}_x=\begin{Bmatrix} f_{x_1} \\ f_{x_2} \\ f_{x_3} \end{Bmatrix},\quad \mathbf{f}_y=\begin{Bmatrix} f_{y_1} \\ f_{y_2} \\ f_{y_3} \end{Bmatrix} \tag{2}$$

3.1. The principal equations

The foregoing EOM are recast in terms of d'Alembert's forces ($\mathbf{f}^D$) by treating the inertial forces as if they are part of the applied forces:

$$\mathbf{f}^D=\begin{Bmatrix} \mathbf{f}_\mathbf{x}^D \\ \mathbf{f}_\mathbf{y}^D \end{Bmatrix}=\begin{Bmatrix} \mathbf{f}_x-\mathbf{m}\ddot{\mathbf{u}}-\mathbf{k}_x\mathbf{u} \\ \mathbf{f}_y-\mathbf{m}\ddot{\mathbf{v}}-\mathbf{k}_y\mathbf{v} \end{Bmatrix} \tag{3}$$

Translational and rotational balance can be further studied by collecting and adding up force and moment components. In the sequel matrix symbols $\mathbf{S}_x^{\mathrm{T}}$, $\mathbf{S}_y^{\mathrm{T}}$, and $\mathbf{S}_\theta^{\mathrm{T}}$ will stand for the summation operators about x, y, and the rotation angle $\theta\equiv\theta_z$ about z, respectively. (The use of the transpose is for convenience in stating the static-kinematic duality discussed later.) For the (x, y) translational force balance we obtain

$$\begin{aligned} &\mathbf{S}_x^{\mathrm{T}}\mathbf{f}_x^D=\mathbf{f}_x^{\mathrm{ext}}-M\ddot{\mathbf{u}}_c=0 \quad \text{with } \mathbf{S}_x^{\mathrm{T}}=[1\ \ 1\ \ 1],\quad M=(m_1+m_2+m_3) \\ &\mathbf{f}_x^{\mathrm{ext}}=(f_{x_1}+f_{x_2}+f_{x_3}),\quad \ddot{\mathbf{u}}_c=(m_1\ddot{u}_1+m_2\ddot{u}_2+m_3\ddot{u}_3)/M \end{aligned} \tag{4}$$

$$\begin{aligned} &\mathbf{S}_y^{\mathrm{T}}\mathbf{f}_y^D=\mathbf{f}_y^{\mathrm{ext}}-M\ddot{\mathbf{v}}_c=0 \quad \text{with } \mathbf{S}_y^{\mathrm{T}}=[1\ \ 1\ \ 1],\quad M=(m_1+m_2+m_3) \\ &\mathbf{f}_y^{\mathrm{ext}}=(f_{y_1}+f_{y_2}+f_{y_3}),\quad \ddot{\mathbf{v}}_c=(m_1\ddot{v}_1+m_2\ddot{v}_2+m_3\ddot{v}_3)/M \end{aligned} \tag{5}$$

For the angular moment balance about the mass center, denoting by $\ddot{\theta}$, the rigid angular acceleration:

$$
\begin{aligned}
M_c^D &= \mathbf{S}_\theta^{\mathrm{T}} \begin{Bmatrix} \mathbf{f}_{\mathbf{x}}^D \\ \mathbf{f}_{\mathbf{y}}^D \end{Bmatrix} = \mathbf{M}^{\mathrm{ext}} - J\ddot{\theta} = 0 \quad \text{with} \\
\mathbf{S}_\theta^{\mathrm{T}} &= [-y_{1c} \;\; -y_{2c} \;\; -y_{3c} \;\; x_{1c} \;\; x_{2c} \;\; x_{3c}], \quad x_{ic} = x_i - x_c, \text{ etc.} \\
\mathbf{M}^{\mathrm{ext}} &= \mathbf{S}_\theta^{\mathrm{T}} \begin{Bmatrix} \mathbf{f}_x^{\mathrm{ext}} \\ \mathbf{f}_y^{\mathrm{ext}} \end{Bmatrix}, \quad J = \sum_{i=1}^{3} m_i (x_{ic}^2 + y_{ic}^2) \\
\begin{Bmatrix} \ddot{u}_i \\ v_i \end{Bmatrix} &= \begin{Bmatrix} \ddot{\mathbf{u}}_c \\ \ddot{\mathbf{v}}_c \end{Bmatrix} + \begin{Bmatrix} -y_{ic} \\ x_{ic} \end{Bmatrix} \ddot{\theta}, \quad \sum_{i=1}^{3} m_i y_{ic} = 0, \quad \sum_{i=1}^{3} m_i x_{ic} = 0
\end{aligned}
\tag{6}
$$

Note that the summation operators cancel out the internal spring forces. This can be seen by introducing the internal force vector:

$$
\mathbf{S}_x^{\mathrm{T}} \mathbf{f}_x^{\mathrm{int}} = 0, \quad \mathbf{S}_y^{\mathrm{T}} \mathbf{f}_y^{\mathrm{int}} = 0, \quad \mathbf{S}_\theta^{\mathrm{T}} \begin{Bmatrix} \mathbf{f}_x^{\mathrm{int}} \\ \mathbf{f}_y^{\mathrm{int}} \end{Bmatrix} = 0 \tag{7}
$$

in which $\mathbf{f}_x^{\mathrm{int}} = \mathbf{k}_x \mathbf{u}$ and $\mathbf{f}_y^{\mathrm{int}} = \mathbf{k}_y \mathbf{u}$ are spring forces. Conditions (7) characterize the *self-equilibrium states*, also denoted as 'self-equilibrated states' in the literature. This terminology applies to floating structures or bodies without external or reaction forces. We will refer to $(\mathbf{S}_x^{\mathrm{T}}, \mathbf{S}_y^{\mathrm{T}}, \mathbf{S}_\theta^{\mathrm{T}})$ as the *self-equilibrium operators.* The nontrivial overall balance equations for the example problem (4), (5), (6) will be referred to as *d'Alembert–Lagrange principal equations*, to recognize the pioneering contributions of d'Alembert [35] and Lagrange [33] outlined in the *Historical Background* section. The abbreviation *principal equations* will be often used.

In FEM discretizations, freedoms are arranged node-by-node. This rearrangement can be done by the permutation matrix

$$
\begin{Bmatrix} u_1 \\ v_1 \\ u_2 \\ v_2 \\ u_3 \\ v_3 \end{Bmatrix} = \mathbf{P} \begin{Bmatrix} u_1 \\ u_2 \\ u_3 \\ v_1 \\ v_2 \\ v_3 \end{Bmatrix} = \begin{bmatrix} 1 & & & & & \\ & & & 1 & & \\ & 1 & & & & \\ & & & & 1 & \\ & & 1 & & & \\ & & & & & 1 \end{bmatrix} \begin{Bmatrix} u_1 \\ u_2 \\ u_3 \\ v_1 \\ v_2 \\ v_3 \end{Bmatrix} \tag{8}
$$

where blank entries store zeros. Rearranging freedoms as per $\mathbf{P}$ and the d'Alembert forces as per $\mathbf{f}^D$, Equations (4)–(6) can be compactly expressed as

$$
\mathbf{S}^{\mathrm{T}} \mathbf{f}^D = \mathbf{0} \quad \text{in which } \mathbf{S}^{\mathrm{T}} = \begin{bmatrix} \mathbf{S}_x^{\mathrm{T}} \\ \mathbf{S}_y^{\mathrm{T}} \\ \mathbf{S}_\theta^{\mathrm{T}} \end{bmatrix} = \begin{bmatrix} 1 & 0 & 1 & 0 & 1 & 0 \\ 0 & 1 & 0 & 1 & 0 & 1 \\ -y_{1c} & x_{1c} & -y_{2c} & x_{2c} & -y_{3c} & x_{3c} \end{bmatrix} \tag{9}
$$

where d'Alembert's forces and the self-equilibrium operators are rearranged in accordance with the DOF permutations given in (8).

3.2. Physical interpretation

Plainly the rows of $\mathbf{S}^{\mathrm{T}}$ displayed in (9) are three independent, infinitesimal RBM of the example system. Thus, its transpose $\mathbf{S}$ is an RBM basis matrix as its columns span the space of rigid motions. Actual RBM amplitudes are obtained by using three dimensionless scaling coefficients: α_x, α_y, and α_{rot}, which are collected into the column 3-vector $\boldsymbol{\alpha}$. The actual rigid-body motion is given by $\mathbf{u}_{\mathrm{r}} = \mathbf{S}\boldsymbol{\alpha}$, whereas the associated virtual rigid-body displacements are $\delta\mathbf{u}_{\mathrm{r}} = \mathbf{S}\delta\boldsymbol{\alpha}$. Applying the PVW to the example system yields

$$(\mathbf{f}^D)^{\mathrm{T}}\delta\mathbf{u}_{\mathrm{r}} = \delta\mathbf{u}_{\mathrm{r}}^{\mathrm{T}}\mathbf{f}^D = \delta\boldsymbol{\alpha}^{\mathrm{T}}\mathbf{S}^{\mathrm{T}}\mathbf{f}^D = \mathbf{0} \tag{10}$$

Since $\delta\boldsymbol{\alpha}$ is arbitrary, $\mathbf{S}^{\mathrm{T}}\mathbf{f}^D$ must vanish, which reproduces (9). The relationship is not accidental and can be shown to hold for any floating body, whether flexible or rigid:

The self-equilibrium and rigid-body-basis matrices are the transposes of each other.

This is an instance of a static-kinematic duality: the equilibrium (balance) and kinematic operators are adjoints of each other (transposes in the case of real operators expressed as matrices). Note that the rigid motion basis collected in $\mathbf{S}$ spans, the *infinitesimal RBMs* and not the finite motions. This is evident from the PVW derivation: in the virtual displacement expression $\delta\mathbf{u}_{\mathrm{r}} = \mathbf{S}\delta\boldsymbol{\alpha}$, matrix $\mathbf{S}$ must be 'frozen' at the current configuration so variations in $\delta\boldsymbol{\alpha}$ merely scale that linearization.

The *orthonormalized rigid-body matrix* $\widehat{\mathbf{R}}$ is the column-orthogonalized $\mathbf{S}$ so that $\widehat{\mathbf{R}}^{\mathrm{T}}\widehat{\mathbf{R}} = \mathbf{I}$. In matrix form

$$\widehat{\mathbf{R}} = \mathbf{S}\mathbf{Q}^{-1/2} \quad \text{with } \mathbf{Q} = \mathbf{S}^{\mathrm{T}}\mathbf{S} \tag{11}$$

(In practice the Gram–Schmidt orthogonalization process or the Cholesky decomposition of $\mathbf{Q}$ may be used to produce $\widehat{\mathbf{R}}$ stably as long as $\mathbf{S}$ has full rank.) The RBM motion $\mathbf{u}_{\mathrm{r}} = \mathbf{S}\boldsymbol{\alpha}$ in terms of the $\widehat{\mathbf{R}}$ basis is $\mathbf{u}_{\mathrm{r}} = \widehat{\mathbf{R}}\widehat{\boldsymbol{\alpha}}$, with $\widehat{\boldsymbol{\alpha}} = \mathbf{Q}^{1/2}\boldsymbol{\alpha}$. For the example problem, the columns of $\mathbf{S}$ are already orthogonal if $x_{1c} + x_{2c} + x_{3c} = 0$ and $y_{1c} + y_{2c} + y_{3c} = 0$, which holds if $m_1 = m_2 = m_3$, and all that remains is normalizing columns of $\mathbf{S}$ to unit length. An alternative orthonormalization of $\mathbf{R}$ with respect to the mass matrix is often more convenient in dynamics.

3.3. Including deformations

The principal equations (9) model only rigid motions. As the example system has six DOF, three additional deformation modes must be included. The complete solution can be obtained by the superposition of rigid and deformation motions: $\mathbf{u} = \mathbf{u}_{\mathrm{r}} + \mathbf{u}_{\mathrm{d}}$. These may be extracted from $\mathbf{u}$ using projection:

$$\mathbf{u}_{\mathrm{d}} = \mathbf{P}_r\mathbf{u} = (\mathbf{I} - \widehat{\mathbf{R}}\widehat{\mathbf{R}}^{\mathrm{T}})\mathbf{u}, \quad \mathbf{u}_{\mathrm{r}} = \mathbf{u} - \mathbf{u}_{\mathrm{d}} = \mathbf{S}\boldsymbol{\alpha} = \widehat{\mathbf{R}}\widehat{\boldsymbol{\alpha}} = \widehat{\mathbf{R}}\widehat{\mathbf{R}}^{\mathrm{T}}\mathbf{u} \tag{12}$$

Note that $\widehat{\mathbf{R}}^{\mathrm{T}}\mathbf{P}_r = \mathbf{P}_r\widehat{\mathbf{R}} = \mathbf{0}$. Furthermore $\mathbf{P}_r = \mathbf{P}_r^{\mathrm{T}}$ and $\mathbf{P}_r^2 = \mathbf{P}_r$, showing that $\mathbf{P}_r$ is an symmetric orthogonal projector. Additional mathematical properties of this decomposition are discussed in [53, 54]. Equation (12) may be interpreted by saying that the principal equations act as a kinematic constraint condition on the well-known flexible EOM, which for infinitesimal motions are

$$\mathbf{K}\mathbf{u} + \mathbf{M}\ddot{\mathbf{u}} = \mathbf{f} \tag{13}$$

For the example problem, the principal equations provide half of the total. For a large-scale problem, however, say, $n \gg 10^5$, the principal equations provide at most six degrees of freedom, which is a tiny percentage. Thus, their constraint role can be appreciated. This role is further examined in Section 4 by considering two floating continuum substructures.

3.4. Quasi-static version and the vibration eigenproblem

For applications in which accelerations are given directly or indirectly it is convenient to recast (13) in the quasi-static format

$$\mathbf{K}\mathbf{u} = \mathbf{f}^* \quad \text{with } \mathbf{f}^* = \mathbf{f} - \mathbf{M}\ddot{\mathbf{u}} \tag{14}$$

Here $\mathbf{f}^*$ is called a statically equivalent force. If $\mathbf{K}$ is m-times singular with kernel (null space) spanned by the m columns of $\mathbf{S}$ (or $\mathbf{R}$), $\mathbf{K}\mathbf{u} = \mathbf{f}^*$ is consistent if and only if $\mathbf{S}^{\mathrm{T}}\mathbf{f}^* = \mathbf{0}$ or $\mathbf{R}^{\mathrm{T}}\mathbf{f}^* = \mathbf{0}$. That is, the equivalent forces $\mathbf{f}^*$ must be in self-equilibrium. If that solvability condition is not met, the right-hand side may be projected on the deformational motion space: $\mathbf{f}_d^* = \mathbf{P}_r\mathbf{f}^*$, as explained by Fraeijs de Veubeke [55] and Geradin and Rixen [25]. However, $\mathbf{K}\mathbf{u} = \mathbf{f}_d^*$ may still suffer from a singular $\mathbf{K}$. If $\mathbf{R}$ is known *a priori*, this can be overcome by using a stabilized stiffness:

$$\mathbf{K}_{st}\mathbf{u} = \mathbf{P}_r(\mathbf{f}_d - \mathbf{M}\ddot{\mathbf{u}}) \quad \text{in which } \mathbf{K}_{st} = \mathbf{K} + \widehat{\mathbf{R}}\widehat{\mathbf{R}}^{\mathrm{T}} \text{ has full rank} \tag{15}$$

Explicit formation of $\mathbf{K}_{st}$ will result generally in a full matrix, hindering sparsity in large-scale problems. Sparsity may be retained, however, by using the techniques described in [54], in which the original system (14) is constrained by 'penalty springs' adaptively injected during factorization, and solved for additional right-hand sides. The solution of (15) is formally $\mathbf{u} = \mathbf{F}\mathbf{f}^*$, in which $\mathbf{F} = \mathbf{K}_{st}^{-1}\mathbf{P}_r = \mathbf{P}_r\mathbf{K}_{st}^{-1}$ is called the free–free flexibility. Technically, $\mathbf{F}$ is the Moore–Penrose generalized inverse of $\mathbf{K}$. Because of the projector action $\mathbf{u} = \mathbf{F}\mathbf{f}^*$ will be simply $\mathbf{u}_{\mathrm{d}}$.

An important application is the free-vibrations eigenproblem with $\mathbf{f} = \mathbf{0}$ and $\ddot{\mathbf{u}}_i = \omega_i^2\mathbf{u}_i$. Linear systems of the form $\mathbf{K}\mathbf{u}_{\mathrm{new}} = \mathbf{M}\mathbf{u}_{\mathrm{old}}$ are repeatedly solved in Lanczos or subspace iteration eigensolvers. The stabilized form (15) is of interest should $\widehat{\mathbf{R}}$, which collects eigenvectors for the m zero frequencies, be assembled *a priori* by geometric arguments, and spectral shifting not used.

4. A PARTLY UNCONSTRAINED STRUCTURE

To illustrate the principal equations for a partly unconstrained structure, consider the 4-bar mechanism linkage shown in Figure 2. (This is a generalization of an example from [56, p. 12], in which it is assumed that the bars are rigid.) Bars (1), (2), and (3) have identical lengths L, elastic moduli E, areas A, are pin-jointed at nodes 1–4, and constrained to move on the $\{x, y\}$ plane. Inertial and damping effects are omitted for simplicity. The degrees of freedom are the $\{x, y\}$ displacements of nodes 2 and 3, collected in $\mathbf{u} = [u_{x2}\ u_{y2}\ u_{x3}\ u_{y3}]^{\mathrm{T}}$, with conjugate forces $\mathbf{f} = [f_{x2}\ f_{y2}\ f_{x3}\ f_{y3}]^{\mathrm{T}}$. Superscript 'ext' is used for given external forces. The arrays of bar axial forces and deformational elongations are denoted by $\mathbf{p} = [p^{(1)}\ p^{(2)}\ p^{(3)}]^{\mathrm{T}}$ and $\mathbf{d} = [d^{(1)}\ d^{(2)}\ d^{(3)}]^{\mathrm{T}}$, respectively. We shall use the abbreviations $c = \cos\varphi$ and $s = \sin\varphi$. If $\varphi \neq 0$ there is only one linearized rigid-body mode, which is the only column of $\mathbf{R}$:

$$\mathbf{S} = \mathbf{R} = [-s\ \ -c\ \ -s\ \ c]^{\mathrm{T}} \tag{16}$$

This may be normalized as $\widehat{\mathbf{R}} = \mathbf{R}/\sqrt{2}$. The 1×4 self-equilibrium matrix is $\mathbf{S}^{\mathrm{T}} = \mathbf{R}^{\mathrm{T}}$.

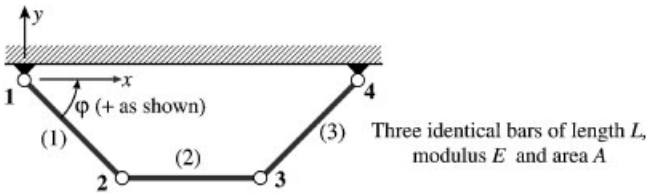

Figure 2. A 4-bar plane mechanism linkage fabricated with three identical bars.

The linearized equilibrium, constitutive and kinematic (deformation–displacement) equations are $\mathbf{B}^{\mathrm{T}}\mathbf{p}=\mathbf{f}$, $\mathbf{p}=\mathbf{C}\mathbf{d}$, and $\mathbf{B}\mathbf{u}=\mathbf{d}$, respectively. Combining them gives the stiffness (of rank 3 if $\varphi\neq 0$): $\mathbf{K}=\mathbf{B}^{\mathrm{T}}\mathbf{C}\mathbf{B}$ that relates $\mathbf{K}\mathbf{u}=\mathbf{f}$:

$$\mathbf{B}=\begin{bmatrix} c & -s & 0 & 0 \\ -1 & 0 & 1 & 0 \\ 0 & 0 & -c & -s \end{bmatrix}, \quad \mathbf{C}=\frac{EA}{L}\mathbf{I}, \quad \mathbf{K}=\frac{EA}{L}\begin{bmatrix} 1+c^2 & -sc & -1 & 0 \\ -sc & s^2 & 0 & 0 \\ -1 & 0 & 1+c^2 & sc \\ 0 & 0 & sc & s^2 \end{bmatrix} \tag{17}$$

Observe that the static-kinematic duality also holds for deformational operators; this is not surprising as the problem is self-adjoint. Given that $\mathbf{S}^{\mathrm{T}}\mathbf{B}^{\mathrm{T}}=\mathbf{0}$ it follows that $\mathbf{S}^{\mathrm{T}}\mathbf{K}=\mathbf{0}$; whence the principal equation is $\mathbf{S}^{\mathrm{T}}\mathbf{f}^{D}=\mathbf{S}^{\mathrm{T}}(\mathbf{f}^{\mathrm{ext}}-\mathbf{K}\mathbf{u})=\mathbf{S}^{\mathrm{T}}\mathbf{f}^{\mathrm{ext}}=-s(f_{x2}^{\mathrm{ext}}+f_{x3}^{\mathrm{ext}})+c(f_{y3}^{\mathrm{ext}}-f_{y2}^{\mathrm{ext}})=0$. This is a self-equilibrium condition that imposes a constraint on the external forces; e.g. any symmetric force system $f_{x2}^{\mathrm{ext}}=-f_{x3}^{\mathrm{ext}}$, $f_{y2}^{\mathrm{ext}}=f_{y3}^{\mathrm{ext}}$ satisfies it for any $\varphi\neq 0$.

The inclusion of inertial and damping terms is straightforward. The case $\varphi=0$, which has two independent linearized RBMs in 2D, requires special treatment and is omitted.

5. MULTIPLIER-CONNECTED FLOATING SUBSTRUCTURES

In this section we consider two substructures resulting from the partition of a semidiscrete, continuum finite element model undergoing 3D motions, as pictured in Figure 3. The model is referred to an inertial coordinate frame (x, y, z) attached to the center of mass. New ingredients with respect to the foregoing example are reaction and interaction forces. Both are treated with Lagrange multipliers. The position, velocity, acceleration, and virtual displacement vectors of a point are given by

$$\begin{aligned} &\mathbf{r}=\mathbf{d}+\mathbf{u}, \quad \mathbf{d}=x\mathbf{i}+y\mathbf{j}+z\mathbf{k}, \quad \mathbf{u}=u\mathbf{i}+v\mathbf{j}+w\mathbf{k} \\ &\dot{\mathbf{r}}=\dot{\mathbf{d}}+\dot{\mathbf{u}}, \quad \dot{\mathbf{d}}=\mathbf{0}, \quad \dot{\mathbf{u}}=\dot{u}\mathbf{i}+\dot{v}\mathbf{j}+\dot{w}\mathbf{k} \\ &\ddot{\mathbf{r}}=\ddot{\mathbf{u}}=\ddot{u}\mathbf{i}+\ddot{v}\mathbf{j}+\ddot{w}\mathbf{k} \\ &\delta\mathbf{r}=\delta u\mathbf{i}+\delta v\mathbf{j}+\delta w\mathbf{k} \end{aligned} \tag{18}$$

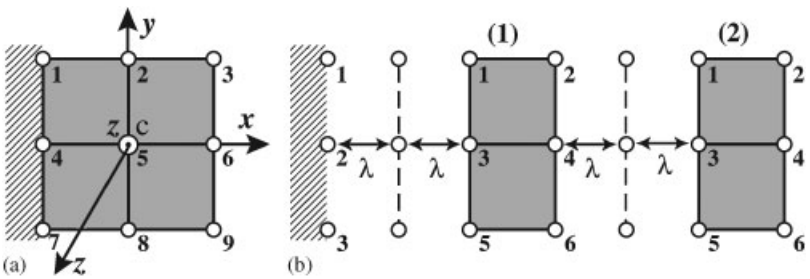

Figure 3. Two floating 3D substructures resulting from partition of a FEM model (the z-direction dimensions are suppressed for visual clarity): (a) assembled structure and (b) partition into two substructures.

Here $(\mathbf{i}, \mathbf{j}, \mathbf{k})$ are fixed unit base vectors attached to the inertial coordinate frame, whereas (u, v, w) are the displacement components. At the six nodal points

$$\mathbf{r}_i = \mathbf{d}_i + \mathbf{u}_i, \quad \mathbf{d}_i = x_i\mathbf{i} + y_i\mathbf{j} + z_i\mathbf{k}, \quad \mathbf{u}_i = u_i\mathbf{i} + v_i\mathbf{j} + w_i\mathbf{k} \ \text{ for } i = 1, 2, 3, \ldots, 6 \tag{19}$$

and similarly for $\dot{\mathbf{r}}_i$, $\ddot{\mathbf{r}}_i$, and $\delta\mathbf{r}_i$. Kinematic node values are collected in vectors $\bar{\mathbf{u}}$, $(\dot{\bar{\mathbf{u}}})$, $(\ddot{\bar{\mathbf{u}}})$ and $\delta(\bar{\mathbf{u}})$, respectively, where the bar distinguishes the node displacements from the field in (19). Volume forces are classified into applied body forces $\mathbf{f}^{\mathrm{E}}$, internal forces $\mathbf{f}^{\mathrm{I}}$ due to elasticity, and inertia force $\rho\ddot{r}$.

Inter-partition interaction as well as ground reactions are treated with Lagrange multipliers λ. These are discretized into delta functions at boundary nodes and collected into a vector $\boldsymbol{\lambda}$. The configuration of this vector depends on details of the treatment of the interaction. Boundary freedoms affected by the interaction are collected in a vector $\mathbf{u}_\lambda = \mathbf{B}_\Gamma\mathbf{u}$ in which $\mathbf{B}_\Gamma$ is a Boolean matrix that extracts $\mathbf{u}_\lambda$ as $\mathbf{B}_\Gamma\mathbf{u}$. To account for possible interpartition dislocations and/or specified support motions the gap vector $\mathbf{u}_{\mathrm{g}}$ is introduced. Application of d'Alembert's principle for the partitioned system gives

$$\delta\Pi = \int_V (\delta\mathbf{r})^{\mathrm{T}}(\mathbf{f}^{\mathrm{ext}} - \mathbf{f}^{\mathrm{I}} - \rho\ddot{\mathbf{r}})\,\mathrm{d}V - \delta\{\boldsymbol{\lambda}^{\mathrm{T}}(\mathbf{B}_\Gamma\bar{\mathbf{u}} - \mathbf{u}_{\mathrm{g}})\} = 0 \tag{20}$$

Substituting (18) and (19) into the above principle, carrying out the spatial integration, we obtain from the stationarity of the above expression:

$$\begin{gathered}
\delta\bar{\mathbf{u}}^{\mathrm{T}}\mathbf{f}^D - \delta\boldsymbol{\lambda}^{\mathrm{T}}\{\mathbf{B}_\Gamma\bar{\mathbf{u}} - \mathbf{u}_{\mathrm{g}}\} = 0, \quad \mathbf{f}^D = \bar{\mathbf{f}}_u^{\mathrm{ext}} - \bar{\mathbf{f}}_u^{\mathrm{I}} - \mathbf{B}_\Gamma^{\mathrm{T}}\boldsymbol{\lambda} - \mathbf{m}_u\ddot{\bar{\mathbf{u}}} \\
\bar{\mathbf{f}}_u^{\mathrm{ext}} = \int_V \mathbf{N}^{\mathrm{T}}\mathbf{f}^{\mathrm{E}}\,\mathrm{d}V, \quad \bar{\mathbf{f}}_u^{\mathrm{I}} = \int_V \mathbf{B}^{\mathrm{T}}\boldsymbol{\sigma}\,\mathrm{d}V, \quad \mathbf{m}_u = \int_V \rho\mathbf{N}^{\mathrm{T}}\mathbf{N}\,\mathrm{d}V \\
\boldsymbol{\varepsilon} = \mathbf{B}\bar{\mathbf{u}}, \quad \mathbf{u} = \sum_{i=1}^{8} \mathbf{N}_i(\xi, \eta, \zeta)\mathbf{u}_i = \mathbf{N}\bar{\mathbf{u}} \\
\bar{\mathbf{u}}^{\mathrm{T}} = [u_1, v_1, w_1, u_2, v_2, w_2, \ldots, u_8, v_8, w_8]
\end{gathered} \tag{21}$$

where $\boldsymbol{\sigma}$ and $\boldsymbol{\varepsilon}$ are stresses and strains, respectively, derived from displacements, $\mathbf{B}$ is the standard strain–displacement relations in the finite element method, and $\mathbf{N}$ are displacement interpolation functions within the brick.

5.1. Principal equations

Adding up d'Alembert forces over all nodes gives

$$\mathbf{S}_{\text{trans}}^{\text{T}}\mathbf{f}^{D}=\mathbf{S}_{\text{trans}}^{\text{T}}\{\bar{\mathbf{f}}_{u}^{\text{ext}}-\mathbf{B}_{\Gamma}^{\text{T}}\boldsymbol{\lambda}-\mathbf{m}_{u}\ddot{\mathbf{u}}\}=\mathbf{0},\quad \text{where } \mathbf{S}_{\text{trans}}^{\text{T}}=\begin{bmatrix}\mathbf{I}_1 & \mathbf{I}_2 & \dots & \mathbf{I}_8\end{bmatrix} \tag{22}$$

where $\mathbf{I}$ is a (3×3) identity matrix and the fact that the internal forces cancel out for a floating structure, viz., $\mathbf{S}_{\text{trans}}^{\text{T}}\bar{\mathbf{f}}_{u}^{\text{I}}=0$, is utilized. The moment summation requires the following vectorial identities:

$$\mathbf{m}_z=\mathbf{r}\times\mathbf{f}=\begin{bmatrix}\mathbf{i}\\ \mathbf{j}\\ \mathbf{k}\end{bmatrix}^{\text{T}}\begin{bmatrix}0 & -z & y\\ z & 0 & -x\\ -y & x & 0\end{bmatrix}\begin{bmatrix}f_x\\ f_y\\ f_z\end{bmatrix},\quad \mathbf{r}=x\mathbf{i}+y\mathbf{j}+z\mathbf{k},\quad \mathbf{f}=f_x\mathbf{i}+f_y\mathbf{j}+f_z\mathbf{k} \tag{23}$$

Let (x_0, y_0, z_0) denote the coordinates of the point about which moments are taken. Defining

$$[\tilde{\mathbf{d}}_i]^{\text{T}}=\begin{bmatrix}0 & -(z_i-z_0) & (y_i-y_0)\\ (z_i-z_0) & 0 & -(x_i-x_0)\\ -(y_i-y_0) & (x_i-x_0) & 0\end{bmatrix} \tag{24}$$

the moment summation can be compactly expressed as

$$\mathbf{S}_{\text{rot}}^{\text{T}}\mathbf{f}^{D}=\mathbf{S}_{\text{rot}}^{\text{T}}\{\bar{\mathbf{f}}_{u}^{\text{ext}}-\mathbf{B}_{\Gamma}^{\text{T}}\boldsymbol{\lambda}-\mathbf{m}_{u}\ddot{\mathbf{u}}\}=0\quad \text{in which } \mathbf{S}_{\text{rot}}^{\text{T}}=[\tilde{\mathbf{d}}_1^{\text{T}}\ \tilde{\mathbf{d}}_2^{\text{T}}\ \dots\ \tilde{\mathbf{d}}_8^{\text{T}}] \tag{25}$$

The sum of moments of the internal forces also vanishes, viz., $\mathbf{S}_{\text{rot}}^{\text{T}}\bar{\mathbf{f}}_{u}^{\text{I}}=0$, regardless of the point about which of the moments are taken.

As discussed in the previous example, the principal Equations (22) and (25) model the admissible rigid-body motions and represent a constraint condition on the interface Lagrange multiplier $\boldsymbol{\lambda}$. This can be seen by writing

$$[\mathbf{S}_{\text{trans}}\ \ \mathbf{S}_{\text{rot}}]^{\text{T}}\mathbf{B}_{\Gamma}^{\text{T}}\boldsymbol{\lambda}=[\mathbf{S}_{\text{trans}}\ \ \mathbf{S}_{\text{rot}}]^{\text{T}}\{\bar{\mathbf{f}}_{u}^{\text{ext}}-\mathbf{m}_{u}\ddot{\mathbf{u}}\} \tag{26}$$

This gives

$$[\mathbf{S}_{\text{trans}}\ \ \mathbf{S}_{\text{rot}}]^{\text{T}}(\mathbf{B}_{\Gamma}^{\text{T}}\boldsymbol{\lambda})-\mathbf{s}=\mathbf{0}\quad \text{whence } \mathbf{s}=[\mathbf{S}_{\text{trans}}\ \ \mathbf{S}_{\text{rot}}]^{\text{T}}\{\bar{\mathbf{f}}_{u}^{\text{ext}}-\mathbf{m}_{u}\ddot{\mathbf{u}}\} \tag{27}$$

Note that $\mathbf{s}=\mathbf{0}$ represents the self-equilibrium equation if the system is completely free. Naturally, for a partitioned system that is a part of constrained system, it represents a violation of the constraint condition.

5.2. Moment summation for structures with rotational freedoms

For structures modeled with rotational degrees of freedom, a modification of the node-by-node force–moment summation is necessary. Assuming that nodal degrees of freedom at node i are

arranged in the usual way: $(u_i, v_i, w_i, \theta_{xi}, \theta_{yi}, \theta_{zi})$ then

$$\mathbf{S}^{\mathrm{T}} = [\mathbf{S}_{\mathrm{trans}} \;\; \mathbf{S}_{\mathrm{rot}}]^{\mathrm{T}} = \begin{bmatrix} \mathbf{S}_1^{\mathrm{T}} & \mathbf{S}_2^{\mathrm{T}} & \dots & \mathbf{S}_n^{\mathrm{T}} \end{bmatrix}$$

$$\mathbf{S}_i^{\mathrm{T}} = \begin{bmatrix} 1 & 0 & 0 & 0 & 0 & 0 \\ 0 & 1 & 0 & 0 & 0 & 0 \\ 0 & 0 & 1 & 0 & 0 & 0 \\ 0 & -(z_i - z_0) & (y_i - y_0) & 1 & 0 & 0 \\ (z_i - z_0) & 0 & -(x_i - x_0) & 0 & 1 & 0 \\ -(y_i - y_0) & (x_i - x_0) & 0 & 0 & 0 & 1 \end{bmatrix} \tag{28}$$

Here (x_0, y_0, z_0) denotes a point around which all the moments are summed up for each given element or each partitioned substructure. These force–moment summation operators can be specialized to models that carry only selective translational and rotational degrees of freedom. For example, for a plane beam with three nodal degrees of freedom, (u, v, θ_z), the node-by-node summation operator is obtained by eliminating the rows and columns corresponding to (w, θ_x, θ_y):

$$\mathbf{S}_i^{\mathrm{T}} = \begin{bmatrix} 1 & 0 & 0 \\ 0 & 1 & 0 \\ -(y_i - y_0) & (x_i - x_0) & 1 \end{bmatrix} \tag{29}$$

Other freedom configurations, such as used in plates and shell models, may be handled similarly.

5.3. Mass properties of arbitrary structures

A trivial yet practically important application of the d'Alembert–Lagrange principal equation is the computations of mass properties of complex geometry. To this end, we introduce the principal mass matrix, $\mathbf{M}_\alpha$, via the virtual work corresponding to the principal inertia force as

$$\begin{aligned} \delta U_r^I &= \delta \mathbf{u}_{\mathrm{r}}^{\mathrm{T}} \mathbf{m}_u \ddot{\mathbf{u}}_{\mathrm{r}}, \quad \mathbf{u}_{\mathrm{r}} = \mathbf{S}\boldsymbol{\alpha} \\ &\Downarrow \\ \delta U_r^I &= \delta \boldsymbol{\alpha}^{\mathrm{T}} \mathbf{M}_\alpha \ddot{\boldsymbol{\alpha}}, \quad \mathbf{M}_\alpha = \mathbf{S}^{\mathrm{T}} \mathbf{m}_u \mathbf{S} \end{aligned} \tag{30}$$

where we employed the summation operator (see Equations (22), (25), and (26)), and the mass matrix($\mathbf{m}_u$) is obtained by the standard FEM procedure. Specifically, $\mathbf{M}_\alpha$ can be expressed as

$$\mathbf{M}_\alpha = \begin{bmatrix} \mathbf{M}_{tt} & \mathbf{m}_{tr} \\ \mathbf{m}_{tr}^{\mathrm{T}} & \mathbf{J}_{rr} \end{bmatrix} \tag{31}$$

where $(\mathbf{M}_{tt}, \mathbf{J}_{rr}, \mathbf{m}_{tr})$ are the (3×3) translational mass, rotatory inertia, and coupling matrix between the translational and rotatory inertia matrix, which vanishes when the center of mass coincides with the point at which the moment self-equilibrium operator, $\mathbf{S}_\alpha$, is generated.

6. STAGED STATIC ANALYSIS

The following example introduces the idea of staged solution of a simple structural system subject to static loads and treated by Lagrange multiplier localization. The general formulation for the dynamic case is provided in the following section.

6.1. The LLM equations

Two fixed-free, parallel extensional springs of axial stiffness k_1 and k_2 that can move only along the x direction are pulled by given static forces as shown in Figure 4. Only x displacements are allowed and thus component subscripts are omitted. Each spring is taken to be a substructure, labeled (1) and (2). Substructures are localized with Lagrange multipliers as illustrated in Figure 4(b). As a result each spring 'floats'. Multipliers are connected to components of a force transducer device called a frame. Figure 4(c) shows the final FEM model with six displacements (four for the springs and two for the frame) and four multipliers. (The following section explains the notation used in Figure 4(c) in more detail.) The FEM model has four element-level stiffness equilibrium equations, four compatibility equations, and two multiplier equilibrium equations. These equations are organized, in that order, to produce the following matrix system, which is displayed both in compact block-matrix notation and in entry-level form:

$$\begin{bmatrix} \mathbf{K} & \mathbf{B} & \mathbf{0} \\ \mathbf{B}^{\mathrm{T}} & \mathbf{0} & -\mathbf{L} \\ \mathbf{0} & -\mathbf{L}^{\mathrm{T}} & \mathbf{0} \end{bmatrix} \begin{Bmatrix} \mathbf{u} \\ \boldsymbol{\lambda} \\ \mathbf{u}_f \end{Bmatrix}$$

$$= \left[\begin{array}{cccc:cccc:c} k_1 & -k_1 & 0 & 0 & 1 & 0 & 0 & 0 & 0 \\ -k_1 & k_1 & 0 & 0 & 0 & 1 & 0 & 0 & 0 \\ 0 & 0 & k_2 & -k_2 & 0 & 0 & 1 & 0 & 0 \\ 0 & 0 & -k_2 & k_2 & 0 & 0 & 0 & 1 & 0 \\ \hdashline 1 & 0 & 0 & 0 & 0 & 0 & 0 & 0 & 0 \\ 0 & 1 & 0 & 0 & 0 & 0 & 0 & 0 & -1 \\ 0 & 0 & 1 & 0 & 0 & 0 & 0 & 0 & 0 \\ 0 & 0 & 0 & 1 & 0 & 0 & 0 & 0 & -1 \\ \hdashline 0 & 0 & 0 & 0 & 0 & -1 & 0 & -1 & 0 \end{array}\right] \begin{Bmatrix} u_1^{(1)} \\ u_2^{(1)} \\ u_1^{(2)} \\ u_2^{(2)} \\ \cdots \\ \lambda_1^{(1)} \\ \lambda_2^{(1)} \\ \lambda_1^{(2)} \\ \lambda_2^{(2)} \\ \cdots \\ u_2 \end{Bmatrix}$$

$$= \left\{ \begin{array}{c} f_1^{(1)}=0 \\ f_2^{(1)}=F_1 \\ f_1^{(2)}=0 \\ f_2^{(2)}=F_2 \\ \cdots\cdots\cdots \\ 0 \\ 0 \\ 0 \\ 0 \\ \cdots\cdots\cdots \\ f_2=P \end{array} \right\} = \left\{ \begin{array}{c} \mathbf{f} \\ \mathbf{0} \\ \mathbf{f}_f \end{array} \right\} \tag{32}$$

In these matrix equations, the specified frame displacement $u_1 = 0$ has been explicitly removed. Substructure displacements are transformed to deformational–rigid normal coordinates using the modal relations

$$\mathbf{u} = \left\{ \begin{array}{c} u_1^{(1)} \\ u_2^{(1)} \\ u_1^{(2)} \\ u_2^{(2)} \end{array} \right\} = \psi \left[\begin{array}{cc|cc} 1 & 0 & 1 & 0 \\ -1 & 0 & 1 & 0 \\ 0 & 1 & 0 & 1 \\ 0 & -1 & 0 & 1 \end{array} \right] \left\{ \begin{array}{c} q_1^{(1)} \\ q_1^{(2)} \\ \vdots \\ \alpha_1^{(1)} \\ \alpha_1^{(2)} \end{array} \right\} = [\boldsymbol{\Phi} \;\; \mathbf{R}] \left\{ \begin{array}{c} \mathbf{q} \\ \boldsymbol{\alpha} \end{array} \right\} \tag{33}$$

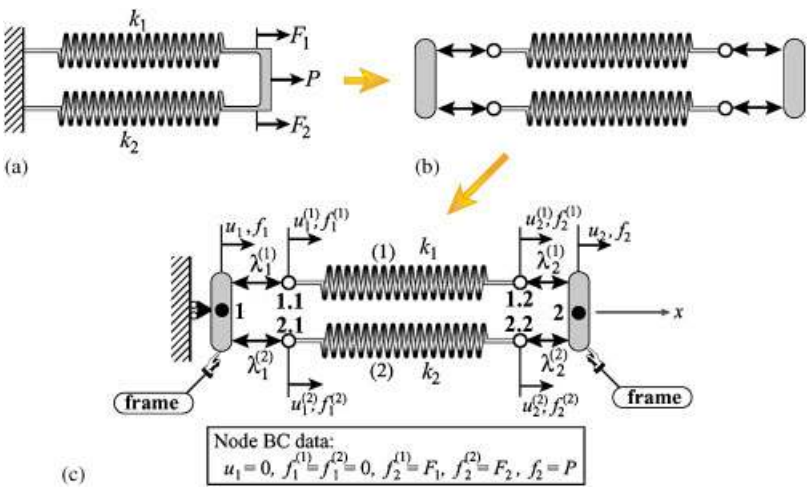

Figure 4. Two linear extensional springs in parallel, localized by Lagrange multipliers: (a) original structure; (b) localization; and (c) FEM model.

in which $\psi = 1/\sqrt{2}$ is a normalization factor. In this equation, $q_i^{(m)}$ and $\alpha_i^{(m)}$ denote deformational and rigid-body motion amplitudes, respectively, for substructure m. Those are collected in separate subvectors $\mathbf{q}$ and $\boldsymbol{\alpha}$. Applying the foregoing transformation to (32) produces the system

$$
\begin{bmatrix} \mathbf{K}_d & \mathbf{0} & \mathbf{B}_d & \mathbf{0} \\ \mathbf{0} & \mathbf{0} & \mathbf{B}_r & \mathbf{0} \\ \mathbf{B}_d^{\mathrm{T}} & \mathbf{B}_r^{\mathrm{T}} & \mathbf{0} & -\mathbf{L} \\ \mathbf{0} & \mathbf{0} & -\mathbf{L}^{\mathrm{T}} & \mathbf{0} \end{bmatrix} \begin{Bmatrix} \mathbf{q} \\ \boldsymbol{\alpha} \\ \boldsymbol{\lambda} \\ \mathbf{u}_f \end{Bmatrix}
$$

$$
= \left[\begin{array}{cc:cc:cccc:c}
2k_1 & 0 & 0 & 0 & \psi & -\psi & 0 & 0 & 0 \\
0 & 2k_2 & 0 & 0 & 0 & 0 & \psi & -\psi & 0 \\ \hdashline
0 & 0 & 0 & 0 & \psi & \psi & 0 & 0 & 0 \\
0 & 0 & 0 & 0 & 0 & 0 & \psi & \psi & 0 \\ \hdashline
\psi & 0 & \psi & 0 & 0 & 0 & 0 & 0 & 0 \\
-\psi & 0 & \psi & 0 & 0 & 0 & 0 & 0 & -1 \\
0 & \psi & 0 & \psi & 0 & 0 & 0 & 0 & 0 \\
0 & -\psi & 0 & \psi & 0 & 0 & 0 & 0 & -1 \\ \hdashline
0 & 0 & 0 & 0 & 0 & -1 & 0 & -1 & 0
\end{array}\right]
\begin{Bmatrix}
q_1^{(1)} \\ q_1^{(2)} \\ \cdots \\ \alpha_1^{(1)} \\ \alpha_1^{(2)} \\ \cdots \\ \lambda_1^{(1)} \\ \lambda_2^{(1)} \\ \lambda_1^{(2)} \\ \lambda_2^{(2)} \\ \cdots \\ u_2
\end{Bmatrix}
$$

$$
= \begin{Bmatrix}
-\psi F_1 \\ -\psi F_2 \\ \vdots \\ \psi F_1 \\ \psi F_2 \\ \vdots \\ 0 \\ 0 \\ 0 \\ 0 \\ \vdots \\ P
\end{Bmatrix} = \begin{Bmatrix} \mathbf{f}_d \\ \mathbf{f}_r \\ \mathbf{0} \\ \mathbf{f}_f \end{Bmatrix} \tag{34}
$$

in which

$$
\mathbf{K}_d = \boldsymbol{\Phi}^{\mathrm{T}} \mathbf{K} \boldsymbol{\Phi}, \quad \mathbf{B}_d = \boldsymbol{\Phi}^{\mathrm{T}} \mathbf{B}, \quad \mathbf{B}_r = \boldsymbol{\Phi}^{\mathrm{T}} \mathbf{R}
$$

6.2. Solution steps

The blocked system (34) will be solved in a hierarchical, step-by-step fashion. The static principal equations are obtained by grouping the second and fourth block-matrix equations, which involve only multipliers:

$$\mathbf{L}_\lambda\boldsymbol{\lambda}=\begin{bmatrix}\mathbf{B}_r\\ -\mathbf{L}^{\mathrm{T}}\end{bmatrix}\boldsymbol{\lambda}=\begin{bmatrix}\psi & \psi & 0 & 0\\ 0 & 0 & \psi & \psi\\ \vdots & \vdots & \vdots & \vdots\\ 0 & -1 & 0 & -1\end{bmatrix}\begin{Bmatrix}\lambda_1^{(1)}\\ \lambda_2^{(1)}\\ \lambda_1^{(2)}\\ \lambda_2^{(2)}\end{Bmatrix}=\begin{Bmatrix}\psi F_1\\ \psi F_2\\ \vdots\\ \underline{\mathrm{P}}\end{Bmatrix}=\begin{Bmatrix}\mathbf{f}_r\\ \mathbf{f}_f\end{Bmatrix}=\mathbf{f}_\lambda \tag{35}$$

Denote by $\mathbf{L}_\lambda^+$ the pseudoinverse of $\mathbf{L}_\lambda$ that satisfies the 4 Penrose conditions, and by $\mathbf{Z}_\lambda$ a basis for the null space of $\mathbf{L}_\lambda$, that is, $\mathbf{L}_\lambda\mathbf{Z}_\lambda=\mathbf{0}$. (If $\mathbf{L}_\lambda$ is square and of full rank, $\mathbf{L}_\lambda^+=\mathbf{L}_\lambda^{-1}$ is the ordinary inverse while $\mathbf{Z}_\lambda$ is void.) The general solution of (35) is the sum of the particular and homogeneous solutions: $\boldsymbol{\lambda}=\mathbf{L}_\lambda^+\mathbf{f}_\lambda+\mathbf{Z}_\lambda\boldsymbol{\beta}$, in which $\boldsymbol{\beta}$ is an array of parameters $\beta_1,\ldots,\beta_k$ of length k equal to the null space dimension of $\mathbf{L}_\lambda$. For the example problem, $k=1$ and

$$\begin{aligned}\boldsymbol{\lambda}&=\begin{Bmatrix}\lambda_1^{(1)}\\ \lambda_2^{(1)}\\ \lambda_1^{(2)}\\ \lambda_2^{(2)}\end{Bmatrix}=\mathbf{L}_\lambda^{-G}\mathbf{f}_\lambda+\mathbf{Z}_\lambda\boldsymbol{\beta}=\frac{1}{2}\begin{bmatrix}3\psi & \psi & 1\\ \psi & -\psi & -1\\ \psi & 3\psi & 1\\ -\psi & \psi & -1\end{bmatrix}\begin{Bmatrix}\psi F_1\\ \psi F_2\\ P\end{Bmatrix}+\begin{bmatrix}1\\ -1\\ -1\\ 1\end{bmatrix}\beta_1\\ &=\frac{1}{4}\begin{Bmatrix}3F_1+F_2+2P\\ F_1-F_2-2P\\ F_1+3F_2+2P\\ -F_1+F_2-2P\end{Bmatrix}+\begin{bmatrix}1\\ -1\\ -1\\ 1\end{bmatrix}\beta_1=\boldsymbol{\lambda}^P+\Delta\boldsymbol{\lambda}\end{aligned} \tag{36}$$

We call $\boldsymbol{\lambda}^P$ the self-equilibrium *principal solution*. If $\boldsymbol{\beta}$ is not void, the correction $\Delta\boldsymbol{\lambda}=\mathbf{Z}_\lambda\boldsymbol{\beta}$ is determined in the next step to account for flexibility and compatibility effects. By construction those two vectors are orthogonal: $\Delta\boldsymbol{\lambda}^{\mathrm{T}}\boldsymbol{\lambda}^P=0$, whence $\boldsymbol{\lambda}^P$ can be interpreted as the l_2 minimum-norm solution of the rigid motion and frame equilibrium equations. Thus, this first step has features in common with the minimum-norm approach to the force method [48, 49]. The major difference is that *no structural flexibilities are involved*: as discussed in the following section $\mathbf{B}_r$ and $\mathbf{L}$ are *purely geometric* matrices, and in fact $\mathbf{L}$ is Boolean.

Inserting $\boldsymbol{\lambda}=\boldsymbol{\lambda}^P+\Delta\boldsymbol{\lambda}$ in the first and third matrix equations and passing the terms involving $\boldsymbol{\lambda}^P$ to the RHS gives the symmetric system

$$\begin{aligned}\begin{bmatrix}\mathbf{K}_d & \mathbf{B}_d\mathbf{Z}_\lambda\\ \mathbf{Z}_\lambda^{\mathrm{T}}\mathbf{B}_d^{\mathrm{T}} & \mathbf{0}\end{bmatrix}\begin{Bmatrix}\mathbf{q}\\ \boldsymbol{\beta}\end{Bmatrix}&=\begin{bmatrix}2k_1 & 0 & \sqrt{2}\\ 0 & 2k_2 & -\sqrt{2}\\ \sqrt{2} & -\sqrt{2} & 0\end{bmatrix}\begin{Bmatrix}q_1^{(1)}\\ q_1^{(2)}\\ \beta_1\end{Bmatrix}\\ &=-\frac{1}{2\sqrt{2}}\begin{Bmatrix}3F_1+F_2+2P\\ -F_1+3F_2+2P\\ 0\end{Bmatrix}=\begin{Bmatrix}\mathbf{f}_d-\mathbf{B}_d\boldsymbol{\lambda}^P\\ \mathbf{0}\end{Bmatrix}\end{aligned} \tag{37}$$

Solving yields

$$\begin{Bmatrix} q_1^{(1)} \\ q_1^{(2)} \\ \beta_1 \end{Bmatrix} = \frac{1}{4(k_1+k_2)} \begin{Bmatrix} -2\sqrt{2}(F_1+F_2+P) \\ -2\sqrt{2}(F_1+F_2+P) \\ (k_1-3k_2)F_1+(3k_1-k_2)F_2+2(k_1-k_2)P \end{Bmatrix} \tag{38}$$

Replacing β_1 in (36) furnishes the final form of the Lagrange multipliers

$$\boldsymbol{\lambda} = \begin{Bmatrix} \lambda_1^{(1)} \\ \lambda_2^{(1)} \\ \lambda_1^{(2)} \\ \lambda_2^{(2)} \end{Bmatrix} = \boldsymbol{\lambda}^P + \Delta\boldsymbol{\lambda} = \frac{1}{k_1+k_2} \begin{Bmatrix} k_1(F_1+F_2+P) \\ k_2F_1-k_1(F_2+P) \\ k_2(F_1+F_2+P) \\ -k_2(F_1+P)+k_1F_2 \end{Bmatrix} \tag{39}$$

If computation of rigid body motion amplitudes and frame displacements is of no interest, as is occasionally the case in static analysis, the solution process may stop here. Else one proceeds to the third step, taking the compatibility equations: $\mathbf{B}_d\mathbf{q}+\mathbf{B}_r\boldsymbol{\alpha}-\mathbf{L}\mathbf{u}_f=\mathbf{0}$, plugging in $\mathbf{q}$ from the second step, and solving for $\boldsymbol{\alpha}$ and $\mathbf{u}_f$. Finally, $\mathbf{q}$ and $\boldsymbol{\alpha}$ may be substituted in (33) to recover physical displacements. For this example

$$\begin{Bmatrix} \alpha_1^{(1)} \\ \alpha_1^{(2)} \\ u_2 \end{Bmatrix} = \frac{1}{k_1+k_2} \begin{Bmatrix} (F_1+F_2+P)/\sqrt{2} \\ (F_1+F_2+P)/\sqrt{2} \\ F_1+F_2+P \end{Bmatrix}$$

$$\begin{Bmatrix} u_1^{(1)} \\ u_2^{(1)} \\ u_1^{(2)} \\ u_2^{(2)} \end{Bmatrix} = \frac{1}{\sqrt{2}} \begin{bmatrix} 1 & 0 & 1 & 0 \\ -1 & 0 & 1 & 0 \\ 0 & 1 & 0 & 1 \\ 0 & -1 & 0 & 1 \end{bmatrix} \begin{Bmatrix} q_1^{(1)} \\ q_1^{(2)} \\ \alpha_1^{(1)} \\ \alpha_1^{(2)} \end{Bmatrix} = \begin{Bmatrix} 0 \\ u_2 \\ 0 \\ u_2 \end{Bmatrix} \tag{40}$$

The foregoing three solution steps are flowcharted in Figure 5. It is highlighted there that the second step, which in large-scale problems accounts for the bulk of the computations, is readily parallelized since substructures, as well as supports treated as interfaces, are fully localized by the presence of the Lagrange multipliers.

The explicit reduction to substructural normal coordinates as displayed in Equation (34) was done here for exposition convenience. In actual large-scale implementations only the precalculation of the RBM basis $\mathbf{R}$ is necessary. Efficient preconditioned CG techniques may be used to solve (34) in parallel processing. The key observation is that once $\mathbf{q}$ is eliminated in (34) we can iteratively solve for $\boldsymbol{\lambda}$ with the principal solution (35) as starting vector. In subsequent CG iterations, new iterates (as defined by $\boldsymbol{\beta}^k$ at the kth iteration) are projected onto the principal solution basis $\mathbf{L}_\lambda^{-G}$; hence,

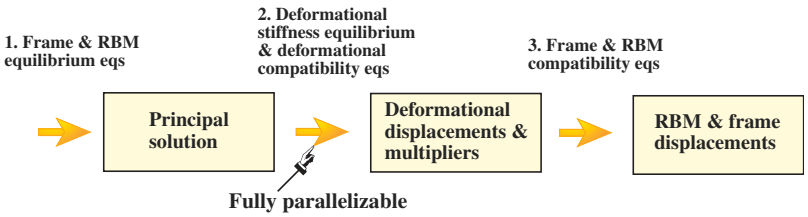

Figure 5. Computational sequence followed in static analysis.

subsequent iterates are orthogonal to the principal solution, i.e. they are purely deformational. Details of this solution procedure may be found in [3, 27].

7. DISCRETE VARIATIONAL FORMULATION

This section extends the example-oriented derivations of the foregoing sections to a more general case: a linear elastic structure partitioned into N substructures, each discretized by FEM. Damping effects are ignored. Substructure meshes are assumed to match across interfaces. (The case of nonmatching meshes is more elaborate although it can be treated by similar methods; the reader is referred to [57–59] for details.)

To illustrate the notation introduced below, reference is often made to Figures 6 and 7. The 2D finite element mesh of Figure 6(a) is divided into three substructures: Σ^1, Σ^2, and Σ^3 by the cuts shown in Figure 6(b). The supported (displacement prescribed) portion of the boundary is also cut off; hence, the three partitions are completely unconstrained. Nodes located along the cuts are called interface nodes. DOF allocated to interface nodes are called interface freedoms. Interface nodes are marked by $\oplus$ in Figure 6(c). Substructure nodes not located on interfaces are called *internal*; those are marked by $\bigcirc$ in Figure 6(c).

A kinematic frame is inserted between substructure interfaces as well as between substructures and supports. This is illustrated in Figure 6(c), in which meshes, supports, and frame are drawn slightly offset as an aid to visualization. The frame is a purely geometric object placed over element sides (in 2D) or faces (in 3D). Unlike contact, fracture, or interface elements, it is not endowed with physical properties. For matching meshes, frame nodes are collocated with interfaced nodes.

The main purpose of the frame is to completely localize partition information, including interface forces. To this end, frame and interface nodes are linked with Lagrange multipliers as shown in Figure 6(c). Mathematically the multipliers are node-collocated delta functions whereas physically they are interface node forces. Choice of this discretization space circumvents the need to carry out integrals over interfaces.

Figure 7 shows global and local node identification. In the latter, nodes are labeled by an integer pair (i, n) that identifies the nth node of the ith partition; those are marked as $i.n$ in Figure 7(b) for ease of reading. The frame is conventionally given index zero so $(0, n)$ is simply shown as n there. When labeling node freedoms, the substructure index is placed as superscript for visualization convenience. Thus, $u^{(3)}_{x_7}$ denotes the x displacement of node 7 of substructure 3. Frame nodes may be labeled with subscript f if this helps to clarify the notation; for example, $\mathbf{u}_{f_7}$ denotes the subvector of node displacements of frame node 7.

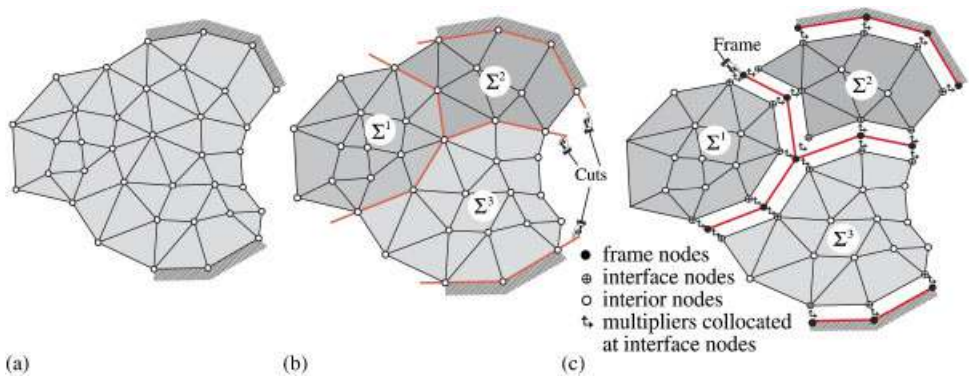

Figure 6. Partition of a finite element mesh into 3 node-matching floating substructures, followed by introduction of interface frame and Lagrange multiplier connectors.

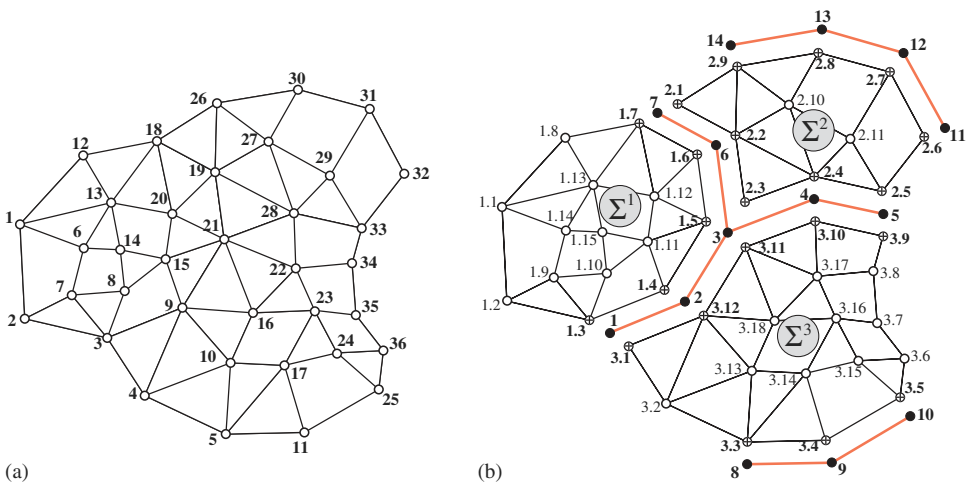

Figure 7. Global and local node labeling.

In superelement-like, multilevel versions of this approach (not considered here) a triplet (l, i, n) including a superelement level index l would be required for substructures, and a duplex for interface frames.

7.1. Localization

If all substructures are collectively assembled into a single structure, as in Figure 6(a), the overall node displacement vector, node velocity vector, node acceleration vector, node force vector, stiffness matrix, and mass matrix are denoted by $\mathbf{u}_g$, $\dot{\mathbf{u}}_g$, $\ddot{\mathbf{u}}_g$, $\mathbf{f}_g$, $\mathbf{K}_g$, and $\mathbf{M}_g$, respectively. The corresponding entities for substructure m are called $\mathbf{u}^{(m)}$, $\dot{\mathbf{u}}^{(m)}$, $\ddot{\mathbf{u}}^{(m)}$, $\mathbf{f}^{(m)}$, $\mathbf{K}^{(m)}$, and $\mathbf{M}^{(m)}$ for $m = 1, 2, \ldots, N$, respectively. Symbols $\mathbf{K}$ and $\mathbf{M}$, without superscripts, denote the block-diagonal matrices built up

with the disconnected stiffness and mass matrices:

$$\mathbf{K}=\text{diag}[\mathbf{K}^{(1)},\mathbf{K}^{(2)},\ldots,\mathbf{K}^{(N)}],\quad \mathbf{M}=\text{diag}[\mathbf{M}^{(1)},\mathbf{M}^{(2)},\ldots,\mathbf{M}^{(N)}] \tag{41}$$

Symbols $\mathbf{u}$ and $\mathbf{f}$, without subscripts, denote the vector concatenation of the $\mathbf{u}^{(m)}$ and $\mathbf{f}^{(m)}$, respectively. The substructure and global discretization levels are formally connected by Boolean matrices and are defined as

$$\begin{Bmatrix}\mathbf{u}^{(1)}\\ \mathbf{u}^{(2)}\\ \vdots\\ \mathbf{u}^{(N)}\end{Bmatrix}=\begin{bmatrix}\mathbf{L}^{(1)}\\ \mathbf{L}^{(2)}\\ \vdots\\ \mathbf{L}^{(N)}\end{bmatrix}\mathbf{u}_{\text{g}},\quad [(\mathbf{L}^{(1)})^{\text{T}}\ \ (\mathbf{L}^{(2)})^{\text{T}}\ \ \ldots\ \ (\mathbf{L}^{(N)})^{\text{T}}]\begin{Bmatrix}\mathbf{f}^{1}\\ \mathbf{f}^{2}\\ \vdots\\ \mathbf{f}^{(N)}\end{Bmatrix}=\mathbf{f}_{\text{g}} \tag{42}$$

These can be compactly written as the supermatrix relations

$$\mathbf{u}=\mathbf{L}\mathbf{u}_{\text{g}},\quad \mathbf{L}^{\text{T}}\mathbf{f}=\mathbf{f}_{\text{g}} \tag{43}$$

The substructure-by-substructure assembly operation may be expressed as the congruences

$$\mathbf{K}_{\text{g}}=\mathbf{L}^{\text{T}}\mathbf{K}\mathbf{L},\quad \mathbf{M}_{\text{g}}=\mathbf{L}^{\text{T}}\mathbf{M}\mathbf{L},\quad \mathbf{f}_{\text{g}}=\mathbf{L}^{\text{T}}\mathbf{f} \tag{44}$$

although these entities are never actually assembled. For each substructure, we identify a subset $\mathbf{u}_{\text{b}}^{(m)}$ $(m=1,2,\ldots,N)$ of *interface degrees of freedom*, in which subscript b stands for 'boundary'. (For substructures subjected to support or contact constraints that subset includes such freedoms if those constraints are treated by Lagrange multipliers as in Figure 6(c).) Interface DOFs are extracted by the matrix operation $\mathbf{u}_{\text{b}}^{(m)}=\mathbf{B}^{(m)}\mathbf{u}^{(m)}$, where $\mathbf{B}^{(m)}$ is a *boundary localization* Boolean matrix. Symbols $\mathbf{B}$ and $\mathbf{u}_{\text{b}}$ without superscripts, denote

$$\mathbf{u}_{\text{b}}=[\mathbf{u}_{\text{b}}^{1}\ \ \mathbf{u}_{\text{b}}^{2}\ \ \ldots\ \ \mathbf{u}_{\text{b}}^{N}],\quad \mathbf{B}=\text{diag}[\mathbf{B}_{\text{b}}^{1}\ \ \mathbf{B}_{\text{b}}^{2}\ \ \ldots\ \ \mathbf{B}_{\text{b}}^{N}]\quad \text{whence } \mathbf{u}_{\text{b}}=\mathbf{B}_{\text{b}}\mathbf{u}_{\text{g}} \tag{45}$$

Frame displacements are collected in vector $\mathbf{u}_f$. These will be considered as *independent variables* in the partitioned approach. Finally, we introduce N localization matrices $\mathbf{B}_f^{(m)}$ that link the frame displacements $\mathbf{u}_f$ to the interface freedoms of the mth substructure as

$$\mathbf{u}_{\text{b}}^{(m)}=\mathbf{B}_f^{(m)}\mathbf{u}_f,\quad m=1,2,\ldots,N \text{ and collectively } \mathbf{u}_{\text{b}}=\mathbf{B}_f\mathbf{u}_f \tag{46}$$

7.2. Constraint treatment

The displacements of, say, frame node 2 and partition nodes 1.4 and 3.12 in Figure 7(b) must be the same. In a plane stress problem, this requires four constraints: $u^1_{x4}=u^3_{x12}=u_{x2}$ and $u^1_{y4}=u^3_{y12}=u_{y2}$. Accordingly, four Lagrange multipliers: λ^1_{x4}, λ^3_{x12}, $\lambda^1_{y0.4}$, and λ^3_{y12} are introduced. Their contribution to the energy functional is

$$\lambda^1_{x4}(u^1_{x4}-u_{x2})+\lambda^3_{x12}(u^3_{x12}-u_{x2})+\lambda^1_{y4}(u^1_{y4}-u_{y2})+\lambda^3_{y12}(u^3_{y12}-u_{y2}) \tag{47}$$

Note that multipliers are simply identified by the interface node label. The linkage to a specific frame node is fortuitous: it happens because we consider here only matching meshes.

Multipliers are inserted for each interface node. Those pertaining to substructure m are collected in vector $\boldsymbol{\lambda}^{(m)}$. This has the same length and arrangement as $\mathbf{u}_{\mathrm{b}}^{(m)}$ and consequently the dot product $(\boldsymbol{\lambda}^{(m)})^{\mathrm{T}}\mathbf{u}_{\mathrm{b}}^{(m)}$ exists. All multipliers are collected in vector $\boldsymbol{\lambda}$. The energy contribution of all multipliers can be compactly expressed as

$$\Pi_d = \boldsymbol{\lambda}^{\mathrm{T}}(\mathbf{u}_{\mathrm{b}} - \mathbf{B}_f \mathbf{u}_f) \tag{48}$$

This will be referred to as the *interface energy potential*. (Some authors, such as Fraeijs de Veubeke, call it a 'dislocation energy' following Friedrichs, who introduced the idea of 'constraint relaxation' in a different context.)

7.3. Equations of motion

The d'Alembert force vectors with damping ignored are $\mathbf{f}_{\mathrm{g}}^D = \mathbf{f}_{\mathrm{g}} - \mathbf{K}_{\mathrm{g}}\mathbf{u}_{\mathrm{g}} - \mathbf{M}_{\mathrm{g}}\ddot{\mathbf{u}}_{\mathrm{g}}$ for the assembly and $(\mathbf{f}_i^D)^{(m)} = \mathbf{f}^{(m)} - \mathbf{K}^{(m)}\mathbf{u}^{(m)} - \mathbf{M}^{(m)}\ddot{\mathbf{u}}^{(m)}$ $(m = 1, 2, \ldots, N)$ for the mth substructure. The displacement-based discrete energy functional are denoted $\Pi = \Pi(\mathbf{u}_{\mathrm{g}})$ for the assembled structure and $\Pi^m = \Pi^m(\mathbf{u}_{\mathrm{g}}^m)$ for each individual substructure. The first variation of the global potential is $\delta\Pi_{\mathrm{g}} = \delta\mathbf{u}_{\mathrm{g}}^{\mathrm{T}}\mathbf{f}_{\mathrm{g}}^D$. Setting this to zero yields the well-known global linear structural dynamics equation

$$\mathbf{M}_{\mathrm{g}}\ddot{\mathbf{u}}_{\mathrm{g}} + \mathbf{K}_{\mathrm{g}}\mathbf{u}_{\mathrm{g}} = \mathbf{f}_{\mathrm{g}} \tag{49}$$

For the partitioned system, the total energy is the sum of that contributed by individual substructures, plus the interface potential

$$\begin{aligned}\Pi(\mathbf{u}_{\mathrm{g}}) &= \sum_{m=1}^{N} \Pi^m(\mathbf{u}^m) + \sum_{m=1}^{N} \boldsymbol{\lambda}^m[(\mathbf{B}^m)^{\mathrm{T}}\mathbf{u}^m - (\mathbf{B}_f^m)^{\mathrm{T}}\mathbf{u}_f] \\ &= \Pi_{\mathrm{g}}(\mathbf{u}_{\mathrm{g}}) + \boldsymbol{\lambda}^m[\mathbf{B}^{\mathrm{T}}\mathbf{u}^m - \mathbf{B}_f^{\mathrm{T}}\mathbf{u}_f]\end{aligned} \tag{50}$$

In this functional $\mathbf{u}$, $\mathbf{u}_f$, and $\boldsymbol{\lambda}$ are considered as independent variables and are varied independently. The first variation is

$$\delta\Pi(\mathbf{u}, \mathbf{u}_f, \boldsymbol{\lambda}) = \delta\mathbf{u}^{\mathrm{T}}\mathbf{f}^D + \delta\{\boldsymbol{\lambda}^{\mathrm{T}}(\mathbf{B}^{\mathrm{T}}\mathbf{u} - \mathbf{L}_f\mathbf{u}_f)\} \tag{51}$$

Setting the variation to zero yields the EOM

$$\begin{bmatrix} \mathbf{K} & \mathbf{B} & \mathbf{0} \\ \mathbf{B}^{\mathrm{T}} & \mathbf{0} & -\mathbf{L}_f \\ \mathbf{0} & -\mathbf{L}_f^{\mathrm{T}} & \mathbf{0} \end{bmatrix} \begin{Bmatrix} \mathbf{u} \\ \boldsymbol{\lambda} \\ \mathbf{u}_f \end{Bmatrix} + \begin{bmatrix} \mathbf{M} & \mathbf{0} & \mathbf{0} \\ \mathbf{0} & \mathbf{0} & \mathbf{0} \\ \mathbf{0} & \mathbf{0} & \mathbf{0} \end{bmatrix} \begin{Bmatrix} \ddot{\mathbf{u}} \\ \ddot{\boldsymbol{\lambda}} \\ \ddot{\mathbf{u}}_f \end{Bmatrix} = \begin{Bmatrix} \mathbf{f} \\ \mathbf{0} \\ \mathbf{0} \end{Bmatrix} \tag{52}$$

Note that $\mathbf{K}$, which is a block-diagonal concatenation of singular stiffness matrices as per (41), is highly rank deficient, since its kernel is spanned by the RBMs of all substructures. For example, if $N = 1000$ and each substructure has 6 RBMs, $\mathbf{K}$ will be 6000 times rank deficient. If the EOM (52) are solved by direct time integration, such deficiency is compensated by the presence of the mass matrix. But for certain situations described below, it is convenient to rewrite these equations explicitly in terms of deformational and rigid motions.

7.4. RBM-split EOM

The localized partitioned EOM (52) has full rank, provided the assembled total system Equation (49) has its full rank. However, this rank sufficiency is not adequate when one solves the equation in a partitioned manner. For example, when a subsystem becomes completely free–free as a result of partitioning, its self-equilibrium state (see, e.g. [22]) must be part of the solution. The variational infusion of the self-equilibrium states for all the subsystems can be accomplished by decomposing the subsystem displacement into rigid and deformational: $\mathbf{u}=\mathbf{u}_\mathrm{r}+\mathbf{u}_\mathrm{d}$. These are expressed in modal form $\mathbf{u}_\mathrm{r}=\mathbf{R}\boldsymbol{\alpha}$ and $\mathbf{u}_\mathrm{d}=\boldsymbol{\Phi}\mathbf{q}$, where the modal basis matrices $\mathbf{R}$ and $\boldsymbol{\Phi}$ are orthonormalized with respect to the mass matrix:

$$\Phi^\mathrm{T}\mathbf{M}\Phi=\mathbf{M}_\mathrm{d},\quad \mathbf{R}^\mathrm{T}\mathbf{M}\Phi=\mathbf{0},\quad \mathbf{K}\mathbf{R}=\mathbf{0},\quad \mathbf{R}^\mathrm{T}\mathbf{M}\mathbf{R}=\mathbf{M}_\mathrm{r} \tag{53}$$

in which if the eigenvectors are mass normalized, $\mathbf{M}_\mathrm{d}$ and $\mathbf{M}_\mathrm{r}$ become identity matrices. However, when the RBM are geometrically generated, they are not mass-normalized.

Substitution of $\mathbf{u}=\mathbf{u}_\mathrm{r}+\mathbf{u}_\mathrm{d}=\Phi\mathbf{q}+\mathbf{R}\boldsymbol{\alpha}$ into $\delta\Pi$ (51) gives

$$\delta\Pi(\mathbf{q},\boldsymbol{\alpha},\mathbf{u}_f,\boldsymbol{\lambda}_\ell)=\delta(\Phi\mathbf{q}+\mathbf{R}\boldsymbol{\alpha})^\mathrm{T}\mathbf{f}^D(\Phi\mathbf{q}+\mathbf{R}\boldsymbol{\alpha})+\delta[\boldsymbol{\lambda}^\mathrm{T}(\mathbf{B}^\mathrm{T}(\Phi\mathbf{q}+\mathbf{R}\boldsymbol{\alpha})-\mathbf{L}_f\mathbf{u}_f)] \tag{54}$$

in which $\mathbf{f}^D(\Phi\mathbf{q}+\mathbf{R}\boldsymbol{\alpha})=\mathbf{f}-\mathbf{K}(\Phi\mathbf{q}+\mathbf{R}\boldsymbol{\alpha})-\mathbf{M}(\Phi\ddot{\mathbf{q}}+\mathbf{R}\ddot{\boldsymbol{\alpha}})$.

Setting $\delta\Pi=0$ and exploiting the orthonormality conditions (53) yields the rigid-deformational split EOM:

$$\begin{bmatrix}\mathbf{K}_\mathrm{d} & \mathbf{0} & \mathbf{B}_\mathrm{d} & \mathbf{0}\\ \mathbf{0} & \mathbf{0} & \mathbf{B}_\mathrm{r} & \mathbf{0}\\ \mathbf{B}_\mathrm{d}^\mathrm{T} & \mathbf{B}_\mathrm{r}^\mathrm{T} & \mathbf{0} & -\mathbf{L}_f\\ \mathbf{0} & \mathbf{0} & -\mathbf{L}_f^\mathrm{T} & \mathbf{0}\end{bmatrix}\begin{Bmatrix}\mathbf{q}\\ \boldsymbol{\alpha}\\ \boldsymbol{\lambda}\\ \mathbf{u}_f\end{Bmatrix}+\begin{bmatrix}\mathbf{M}_\mathrm{d} & \mathbf{0} & \mathbf{0} & \mathbf{0}\\ \mathbf{0} & \mathbf{M}_\mathrm{r} & \mathbf{0} & \mathbf{0}\\ \mathbf{0} & \mathbf{0} & \mathbf{0} & \mathbf{0}\\ \mathbf{0} & \mathbf{0} & \mathbf{0} & \mathbf{0}\end{bmatrix}\begin{Bmatrix}\ddot{\mathbf{q}}\\ \ddot{\boldsymbol{\alpha}}\\ \ddot{\boldsymbol{\lambda}}\\ \ddot{\mathbf{u}}_f\end{Bmatrix}=\begin{Bmatrix}\mathbf{f}_\mathrm{d}\\ \mathbf{f}_\mathrm{r}\\ \mathbf{0}\\ \mathbf{0}\end{Bmatrix} \tag{55}$$

in which $\mathbf{K}_\mathrm{d}=\boldsymbol{\Phi}^\mathrm{T}\mathbf{K}\boldsymbol{\Phi}$, $\mathbf{M}_\mathrm{d}=\boldsymbol{\Phi}^\mathrm{T}\mathbf{M}\boldsymbol{\Phi}$, $\mathbf{M}_\mathrm{r}=\mathbf{R}^\mathrm{T}\mathbf{M}\mathbf{R}$, $\mathbf{B}_\mathrm{d}=\boldsymbol{\Phi}^\mathrm{T}\mathbf{B}$, $\mathbf{B}_\mathrm{r}=\mathbf{R}^\mathrm{T}\mathbf{B}$, $\mathbf{f}_\mathrm{d}=\boldsymbol{\Phi}^\mathrm{T}\mathbf{f}$, and $\mathbf{f}_\mathrm{r}=\mathbf{R}^\mathrm{T}\mathbf{f}$. The foregoing matrix equations have immediate physical interpretation: $\mathbf{K}_\mathrm{d}\mathbf{q}+\mathbf{B}_\mathrm{d}\boldsymbol{\lambda}+\mathbf{M}_\mathrm{d}\ddot{\mathbf{q}}=\mathbf{f}_\mathrm{d}$ is the EOM for the substructural deformable modes, $\mathbf{B}_\mathrm{r}\boldsymbol{\lambda}+\mathbf{M}_\mathrm{r}\ddot{\boldsymbol{\alpha}}==\mathbf{f}_\mathrm{r}$ governs substructural rigid motions, $\mathbf{B}_\mathrm{d}^\mathrm{T}\mathbf{q}+\mathbf{B}_\mathrm{r}^\mathrm{T}\boldsymbol{\alpha}-\mathbf{L}_f\mathbf{u}_f=0$ enforces the interface kinematic constraints, and finally $\mathbf{L}_f^\mathrm{T}\boldsymbol{\lambda}=\mathbf{0}$ expresses Newton's third law along the interfaces in terms of LLM. The first and second matrix equations can be *localized* to each substructure since they do not involve the frame displacements $\mathbf{u}_f$ and consequently are fully parallelizable. The only linkage between the localized equations is provided by $\mathbf{u}_f$.

Remark

We have emphasized here the direct construction of self-equilibrium matrix operators (force and moment summation) as basis for building the principal equations. From these, RBM matrices follow by transposition. An alternative procedure is to try to construct the RBM matrices first, either by direct geometric arguments or by computer-based subdomain kinematic analysis based on the singular value decomposition (see, e.g. Farhat and Géradin [60]). The latter technique has the advantage of accounting for the presence of internal mechanisms regardless of their origin (motion-control devices, spurious mesh modes, rank-deficient domain decomposition, etc.). If this alternative strategy is followed, the self-equilibrium conditions again follow from duality. The

mass properties displayed in Equation (31) do not generally hold, however, for null space vectors that are extracted from singular stiffness matrices via an linear algebra procedure.

8. CONCLUSIONS

The focus of the paper has been the application of the d'Alembert–Lagrange principal equations to handle floating mechanical systems or components. As discussed in the *Introduction*, those modeling scenarios may arise directly in naturally unconstrained problems, such as a flying aircraft, or may occur as a result of a system decomposition process. In the latter case, the principal equations become a key ingredient of the formulation of the coupled discrete equations. We have shown that the process relies on PVW applied to the d'Alembert forces acting on the whole system, or on each individual component. Although the procedure can be followed as recipe by practicing engineers without a detailed knowledge of variational principles, work theorems or adjoint properties, such knowledge comes handy in understanding attributes such as the duality between static and kinematic operators.

Two important features of the principal equations presented here are their independence from constitutive and compatibility properties, and their indifference as to the source of forces acting on the system. The latter property represents an extension of the classical notion of 'self-equilibrium states' that refers to structures without external and reaction forces.

If the overall system is statically determinate, the principal equations directly supply the internal forces without the need of finding deformations and displacements. While in static analysis of fully supported structures this feature is common to flexibility-based methods, those cannot easily handle floating systems or dynamics. For statically indeterminate problems, the principal solution may serve as the initial step in an iterative process that injects compatibility and material properties in a hierarchical fashion. That process can be efficiently combined with Lagrange multiplier methods to address scenarios such as multiscale analysis or parallel computation.

As noted in the Historical Background section, multiplier-linked system decomposition methods have diverse roots in the past. In a taxonomy of model-based simulation for computational mechanics, the LLM methodology presented here may be categorized as a primal–dual hybrid: a combination of the displacement and force methods that tries to amalgam the best features of each while retaining application pliability. The following modeling and computational advantages can be cited for this combination.

1. If the system is undecomposed and fully supported, it reduces to the standard direct stiffness method, thus facilitating selective reuse of existing software.
2. At the other extreme, that of widespread cutting of rigid or highly stiff individual members it links naturally to multiplier-based multibody dynamics.
3. For structural models, it uses only displacement-connected elements in each substructure. This protects the large existing investment of commercial FEM codes on element libraries, and retains interelement mixability as the tool to build complex models.
4. Cuts can be placed to evince interaction forces in problems where unexpected highly local effects call for deeper investigation (sort of an 'MRI structural test'). This is important in inverse problems for vulnerability/damage detection suggested by dynamic signal data. A related potential application is real-time, multisite hybrid testing, which is gaining importance as a result of networking advances.

5. Selective elimination of the frame reduces LLM to the mortar method for linking heterogeneous components, allowing result crosschecking with a developing body of multiphysics coupling technology.
6. As emphasized in the paper, the approach naturally handles floating systems and components. Because displacements are an essential part of the formulation, it has no difficulties in modeling dynamics, vibration, and stability problems.
7. In problems that involve localized non-linearities (fracture, contact, etc.), cuts may be adaptively made to separate linear and non-linear portions of the overall system.
8. Lends itself to parallel implementation as well as treatment of nonmatching meshes.
9. It opens up a promising framework for partitioned analysis of coupled problems in multiphysics and multiscale modeling, as well as construction of reduced models by truncated representations of governing equations. Substantial developments in all of these areas, however, will be required to define correct and consistent interface conditions.

Two implementation obstacles remain as research areas that may be of interest to numerical analysts and applied mathematicians. The reliable automatic detection of non-RBM subsystem mechanisms (zero-energy internal modes) is notoriously difficult since it involves rank detection in floating-point arithmetic. Despite recent advances [60], the topic deserves further study. Coupling subsystems or partitions of very different physical or inertial properties can lead to significant ill-conditioning in the interface equations. This can be expected to be particularly crucial in multiscale analysis. While ill-conditioning in structure–structure interaction has been alleviated with *ad hoc* scaling and filtering procedures [61, 62], a more general treatment seems appropriate.

Potential future applications of this approach include situations where noisy large motions, localization, contact-impact, heterogeneity, and/or scaling effects may disturb the smooth application of conventional displacement methods. Specific instances include multiscale inverse problems, space robotics, contact-impact, real-time testing, control of highly flexible systems, and obviously modeling and simulation of multiphysics and multiscale problems.

REFERENCES

1. Shabana AA. *Dynamics of Multibody Systems*. Cambridge University Press: Cambridge, U.K., 1998.
2. Farhat C, Roux FX. A method of finite-element tearing and interconnecting and its parallel solution algorithm. *International Journal for Numerical Methods in Engineering* 1991; **40**:1205–1227.
3. Farhat C, Roux FX. Implicit parallel processing in structural mechanics. *Computational Mechanics Advances* 1994; **2**(1):1–124.
4. Park KC, Felippa CA, Ohayon R. Partitioned formulation of internal fluid–structure interaction problems via localized Lagrange multipliers. *Computer Methods in Applied Mechanics and Engineering* 2001; **190**(24–25): 2989–3007.
5. Ross MR. Coupling and simulation of acoustic fluid–structure interaction systems using localized Lagrange multipliers. *Ph.D. Thesis*, Department of Aerospace Engineering Science, University of Colorado, 2006. Available from: http://caswww.colorado.edu/courses/FSI.d.
6. Frenkel D, Smith B. *Understanding Molecular Simulation*: *From Algorithms to Applications*. Academic Press: San Diego, CA, 2002.
7. Konarev PV, Petoukhov MV, Svergun DI. MASSHA—a graphics system for rigid-body modelling of macromolecular complexes against solution scattering data. *Journal of Applied Crystallography* 2001; **34**:527–532.
8. Nakano A. A rigid-body-based multiple time scale molecular dynamics simulation of nanophase materials. *International Journal of High Performance Computing Applications* 1999; **13**(2):154–162.
9. Pirez J, Faure P, Benoit J-P. Molecular rigid-body displacements in a tetragonal lysozyme crystal confirmed by X-ray diffuse scattering. *Acta Crystallographica* 1996; **D52**:722–729.

10. Sohlberg K, Tuzun RE, Sumpter BG, Noid DW. Application of rigid-body dynamics and semiclassical mechanics to molecular bearings. *Nanotechnology* 1997; **8**:103–111.
11. Dosset P, Hus J-C, Marion D, Blackledge M. A novel interactive tool for rigid-body modeling of multi-domain macromolecules using residual dipolar couplings. *Journal of Biomolecular NMR* 2001; **20**(3):223–231.
12. Knegtel RM, Kuntz ID, Oshiro CM. Molecular docking to ensembles of protein structures. *Journal of Molecular Biology* 1997; **266**:424–440.
13. May A, Eisenhardt S, Schmidt-Ehrenberg J, Cordes F. Rigid body docking for virtual screening. *ZIB-Report 03-47*, Konrad-Zuse-Zentrum für Informationstechnik, Berlin, Germany, 2003.
14. Wang Y, Jernigan RL. Comparison of tRNA motions in the free and ribosomal bound structures. *Biophysical Journal* 2005; **89**:3399–3409.
15. Wriggers W, Schulten K. Protein domain movements: detection of rigid domains and visualization of hinges in comparisons of atomic coordinates. *Proteins* 1997; **29**(1):1–14.
16. Fransen S, Kreis A, Klein M. Rigid body mode control of free–free launcher structural models in gravity fields. *Proceedings of the 45th AIAA/ASME/ASCE/AHS/ASC Structures*, *Structural Dynamics and Materials Conference*, Palm Springs, CA, 19–22 April 2004, Paper No. AIAA 2004-1791.
17. Loper D. On viscous flow within a rotating spheroidal contained. *Quarterly Journal of Mechanics and Applied Mathematics* 1970; **23**(1):119–125.
18. O'Brien JF, Shen C, Gatchalian CM. Synthesizing sounds from rigid-body simulations. *Proceedings of ACM SIGGRAPH Symposium on Computer Animation 2002*, San Antonio, TX, 21–22 July 2002; 175–181.
19. Okuma M, Shi Q. Identification of the principal rigid body modes under free–free boundary condition. *Transactions of ASME Journal of Vibration and Acoustics* 1997; **119**(3):341–345.
20. Argyris JH, Kelsey S. *Energy Theorems and Structural Analysis*. Butterworth: London, 1960; Part I reprinted from *Aircraft Engineering*, vol. 26, October–November 1954 and vol. 27, April–May 1955.
21. Przemieniecki JS. *Theory of Matrix Structural Analysis*. McGraw-Hill: New York, 1968 (Dover edition 1986).
22. Fraeijs de Veubeke BM. Matrix structural analysis. Lecture Notes for the *International Research Seminar on the Theory and Application of Finite Element Methods*, Calgary, Alberta, Canada, July–August 1973; reprinted in *B. M. Fraeijs de Veubeke Memorial Volume of Selected Papers*, Geradin M (ed.). Sitthoff & Noordhoff, Alphen aan den Rijn: The Netherlands, 1980; 509–568.
23. Argyris JH, Mlejnek H-P. *Die Methode der Finiten Elemente*, vols. I–III. Vieweg: Braunschweig, 1986, 1987 and 1988.
24. Verchery G. Régularisation du système de l' équilibre des structures élastiques discrètes. *Comptes Rendus de l'Academie des Sciences Paris* 1990; **311**(II):585–589.
25. Géradin M, Rixen D. *Mechanical Vibrations*: *Theory and Application to Structural Dynamics*. Wiley: New York, 1994.
26. Park KC, Felippa CA. A variational framework for solution method developments in structural mechanics. *Journal of Applied Mechanics* 1998; **65**(1):242–249.
27. Park KC, Justino Jr MR, Felippa CA. An algebraically partitioned FETI method for parallel structural analysis: algorithm description. *International Journal for Numerical Methods in Engineering* 1997; **40**:2717–2737.
28. Park KC, Felippa CA. A variational principle for the formulation of partitioned structural systems. *International Journal for Numerical Methods in Engineering* 2002; **47**:395–418.
29. Park KC, Gumaste U, Felippa CA. A localized version of the method of Lagrange multipliers and its applications. *Computational Mechanics* 2000; **24**(6):476–490.
30. Dugas R. *A History of Mechanics*. Dover Publications: New York, 1988.
31. Truesdell C, Toupin RA. The classical field theories. In *Handbuch der Physik*, vol. III/1, Flügge S (ed.). Springer: Berlin, 1970; 226–790.
32. Lanczos C. *The Variational Principles of Mechanics* (4th edn). Dover: New York, 1986 (1st edn. 1949).
33. Lagrange J-L. *Mécanique Analytique*, Paris, 1788. Reprinted by J. Gabay, Paris, 1989.
34. http://en.wikipedia.org/wiki/Jean_le_Rond_d'Alembert.
35. d'Alembert J, le R. *Traité de Dynamique*, Paris, 1743. Reprinted by Gauthier-Villars: Paris, 1921.
36. Synge JL. Classical dynamics. In *Handbuch der Physik*, vol. III/1, Flügge S (ed.). Springer: Berlin, 1960; 1–225.
37. Newton I. *Philosophiae Naturalis Principia Mathematica* (Mathematical Principles of Natural Philosophy. Also known as the Principia), 1st edn, London, 1687; 2nd edn, Cambridge, 1712; 3rd edn, London 1726, final edn, (prepared by Newton, in English translation by A. Motte), London, 1729.
38. d'Alembert J, le R. *Traité de l'Équilibre et du Mouvement des Fluides pour servir de suite au Traité de Dynamique* (2nd edn). Paris, 1770. Reprinted in 1990 by Jacques Gabay, Sceaux, France.

39. Euler L. Theoria Motus Corporum Solidorum seu Rigidrum ex Primis nostrae Cognitionis Principiis Stabilita et ad Omnis Motus, qui in hujusmodi Corpora Cadere Possunt, 1765. Reprinted in *L. Euler Opera Omnia*, 3D4, 3D293. Natural Science Society: Berne, 1911–1982.
40. Thomson W, Tait PG. *Treatise on Natural Philosophy*, *Part I*. Cambridge University Press: U.K., 1879.
41. Egeland O, Araldsen H. SESAM-69: a general purpose finite element method program. *Computers and Structures* 1974; **4**:41–68.
42. Park KC, Felippa CA. Partitioned analysis of coupled systems. In *Computational Methods for Transient Analysis*, Chapter 3, Belytschko T, Hughes TJR (eds). North-Holland: Amsterdam, 1983; 157–219.
43. Prager W. Variational principles for linear elastostatics for discontinous displacements, strains and stresses. In *Recent Progress in Applied Mechanics*, The Folke-Odgvist Volume, Broger B, Hult J, Niordson F (eds). Almqusit and Wiksell: Stockholm, 1967; 463–474.
44. Tong P. New displacement finite element method for solid continua. *International Journal for Numerical Methods in Engineering* 1970; **2**:73–83.
45. Atluri SN. On 'hybrid' finite-element models in solid mechanics. In *Advances in Computer Methods for Partial Differential Equations*, Vichnevetsky R (ed.). AICA, Rutgers University: New Jersey, 1975; 346–356.
46. Felippa CA. A historical outline of matrix structural analysis: a play in three acts. *Computers and Structures* 2001; **79**:1313–1324.
47. Robinson J. *Structural Matrix Analysis for the Engineer*. Wiley: New York, 1966.
48. Kaneko I, Lawo M, Thierauf G. On computational procedures for the force method. *International Journal for Numerical Methods in Engineering* 1982; **18**:1469–1495.
49. Kaneko I, Plemmons RJ. Minimum norm solutions to linear elastic analysis problems. *International Journal for Numerical Methods in Engineering* 1984; **20**:983–998.
50. Argyris JH, Bronlund OE. The natural factor formulation of the stiffness matrix displacement method. *Computer Methods in Applied Mechanics and Engineering* 1975; **5**:97–119.
51. Patnaik SN. An integrated force method for discrete analysis. *International Journal for Numerical Methods in Engineering* 1973; **6**:237–251.
52. Patnaik SN. The variational energy formulation for the integrated force method. *AIAA Journal* 1986; **24**:129–136.
53. Felippa CA, Park KC, Justino FMR. The construction of free–free flexibility matrices as generalized stiffness inverses. *Computers and Structures* 1997; **88**:411–418.
54. Felippa CA, Park KC. The construction of free–free flexibility matrices for multilevel structural analysis. *Computer Methods in Applied Mechanics and Engineering* 2002; **191**:2111–2140.
55. Fraeijs de Veubeke BM. Iteration in semidefinite eigenvalue problems. *Journal of Astronautical Sciences* 1955; **22**(10):710–720.
56. Kuztesov EN. *Unconstrained Structure Systems*. Springer: New York, 1991.
57. Park KC, Felippa CA, Rebel R. Interfacing nonmatching FEM meshes: the zero moment rule. In *Trends in Computational Structural Mechanics*, Wahl WA, Bletzinger K-U, Schweizerhof K (eds). CIMNE: Barcelona, Spain, 2001; 355–367.
58. Park KC, Felippa CA, Rebel G. A simple algorithm for localized construction of nonmatching structural interfaces. *International Journal for Numerical Methods in Engineering* 2002; **53**:2117–2142.
59. Rebel R, Park KC, Felippa CA. A contact formulation based on localised Lagrange multipliers: formulation and application to two-dimensional problems. *International Journal for Numerical Methods in Engineering* 2002; **54**:263–297.
60. Farhat C, Géradin M. On the general solution by a direct method of a largescale singular system of linear equations: application to the analysis of floating structures. *International Journal for Numerical Methods in Engineering* 1998; **41**:675–696.
61. González LA, Park KC, Felippa CA. Partitioned formulation of frictional contact problems using localized Lagrange multipliers. *Communications in Numerical Methods in Engineering* 2006; **22**:319–333.
62. Park KC, Felippa CA, Caillerie D, Ohayon R. On transforming tight coupling into loose coupling for a class of multiscale models. *Proceedings of Computational Methods in Coupled Problems in Sciences and Engineering*, Ibiza, Spain, 21–23 May 2007.